Introduction to Single-Wall Carbon Nanotubes, and application of SWNTs to PV devices

Carbon single-wall nanotube crystallography

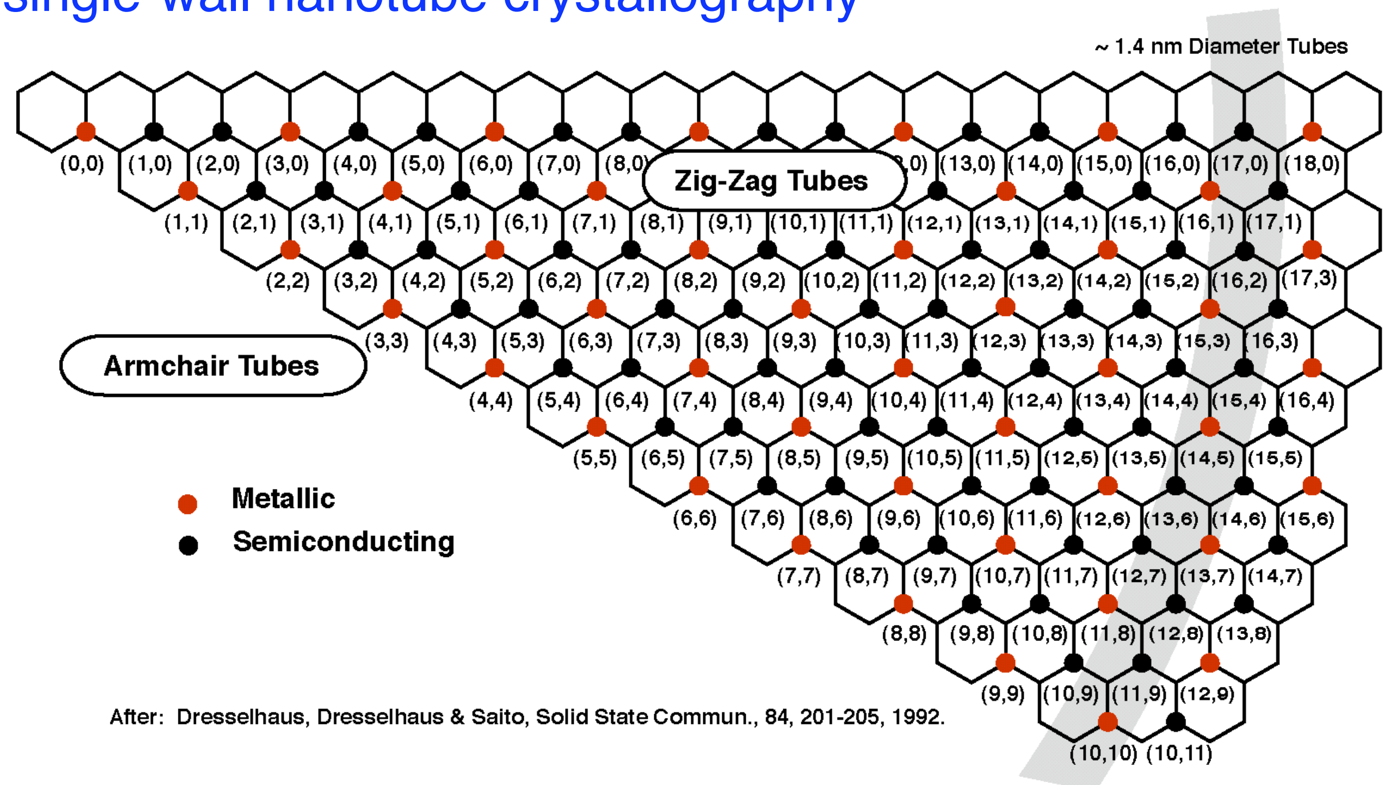

(10,10) - metallic

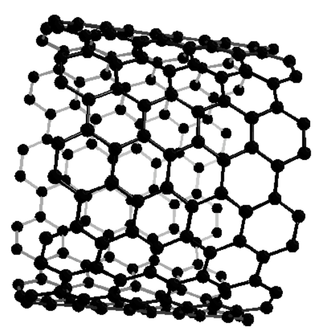

(17,0) - semiconductor

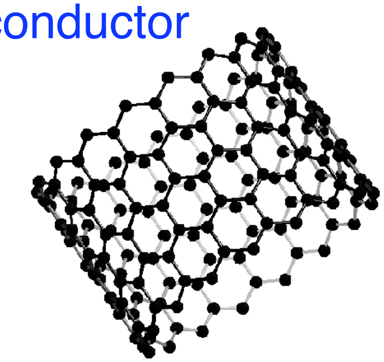

Nanotube Structure in a Nutshell

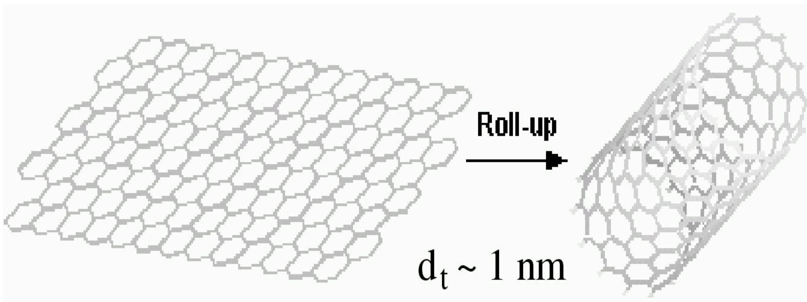

Graphene Sheet **SWNT**

Rolled-up graphene layer
Large unit cell.

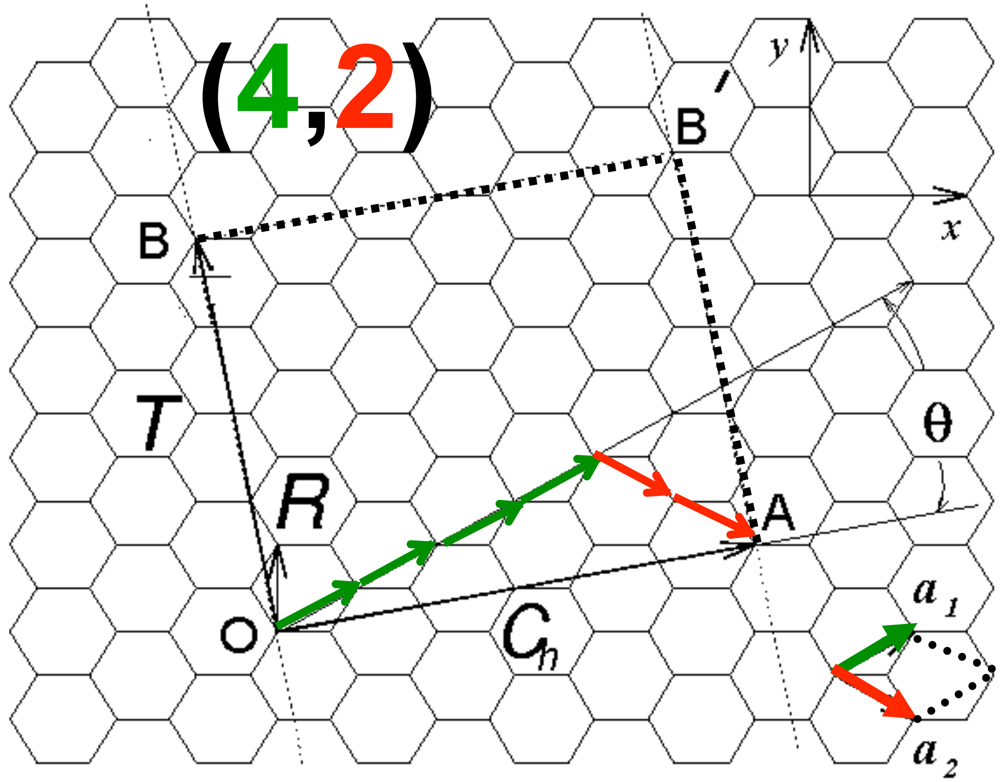

$$\vec{C}_h = n\vec{a}_1 + m\vec{a}_2 \equiv (n,m)$$

$$\begin{cases} d_t = \dfrac{L}{\pi} = \dfrac{a}{\pi}\sqrt{n^2 + nm + m^2} \\ \theta = \tan^{-1}\dfrac{\sqrt{3}m}{2n+m} \end{cases}$$

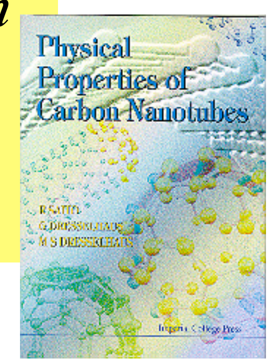

from Dresselhaus

Each (n,m) nanotube is a unique molecule

SWNT synthesis by laser vaporization

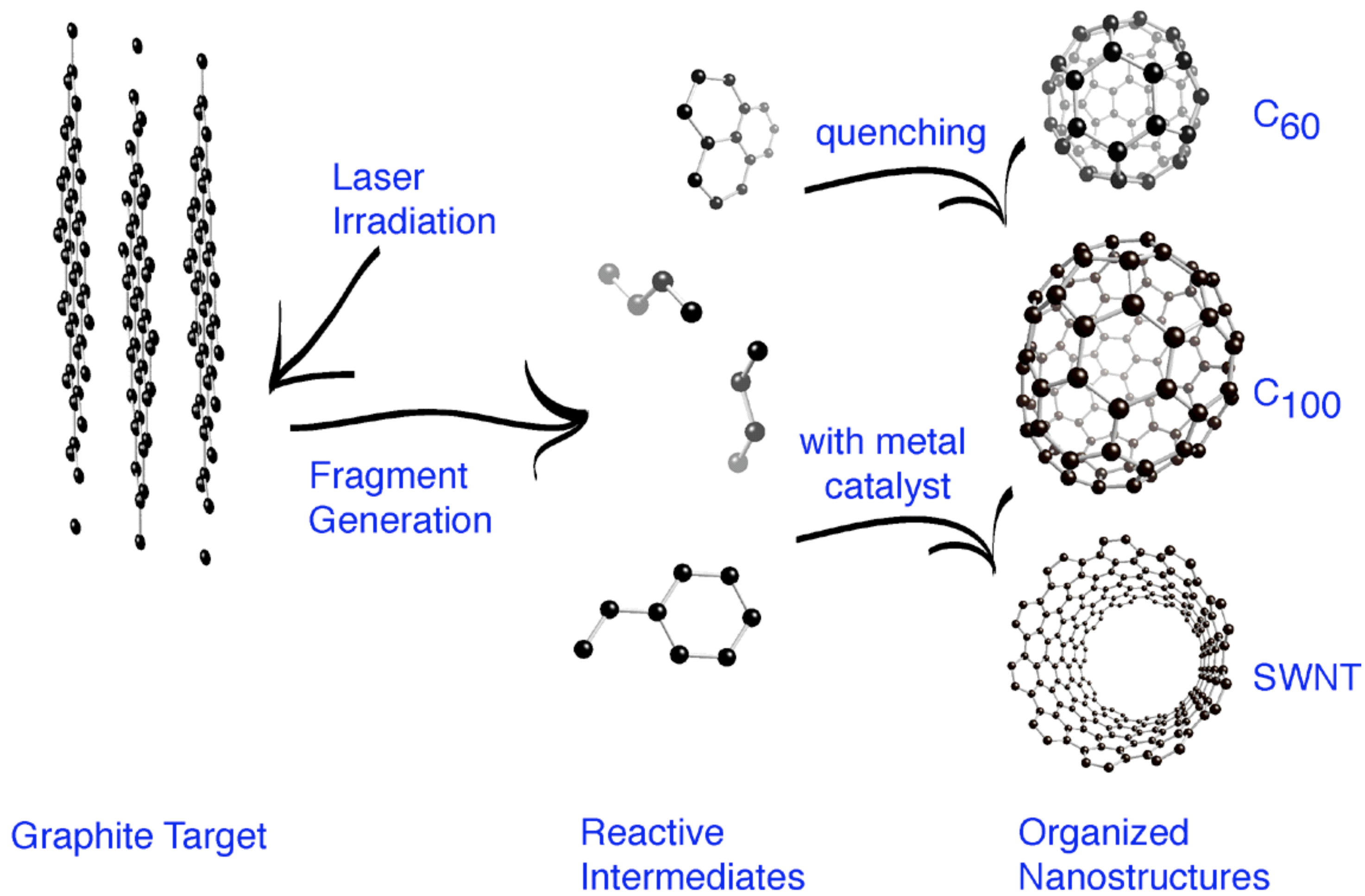

Some milestones in "Carbon Nanoscience"

1985 - R.F. Curl, H.W. Kroto, R.E. Smalley discover C_{60}
(leads to 1996 Nobel Prize in Chemistry).

1990 - Kratschmer et al. produce macroscopic quantities of C_{60}

1991 - Iijima discovers multi-walled carbon nanotubes (MWNTs).

1992 - Ebbesen and Ajayan synthesize gram quantities of MWNTs.

1993 - Iijima & Ichihashi and Bethune et al. simultaneously discover single-wall nanotubes (SWNTs) grown by arc-discharge.

1995 - Guo et al. introduce laser vaporization for production of higher purity SWNT samples.

1996 - Dai et al. decompose CO on metal catalysts to grow SWNTs, introducing chemical vapor deposition.

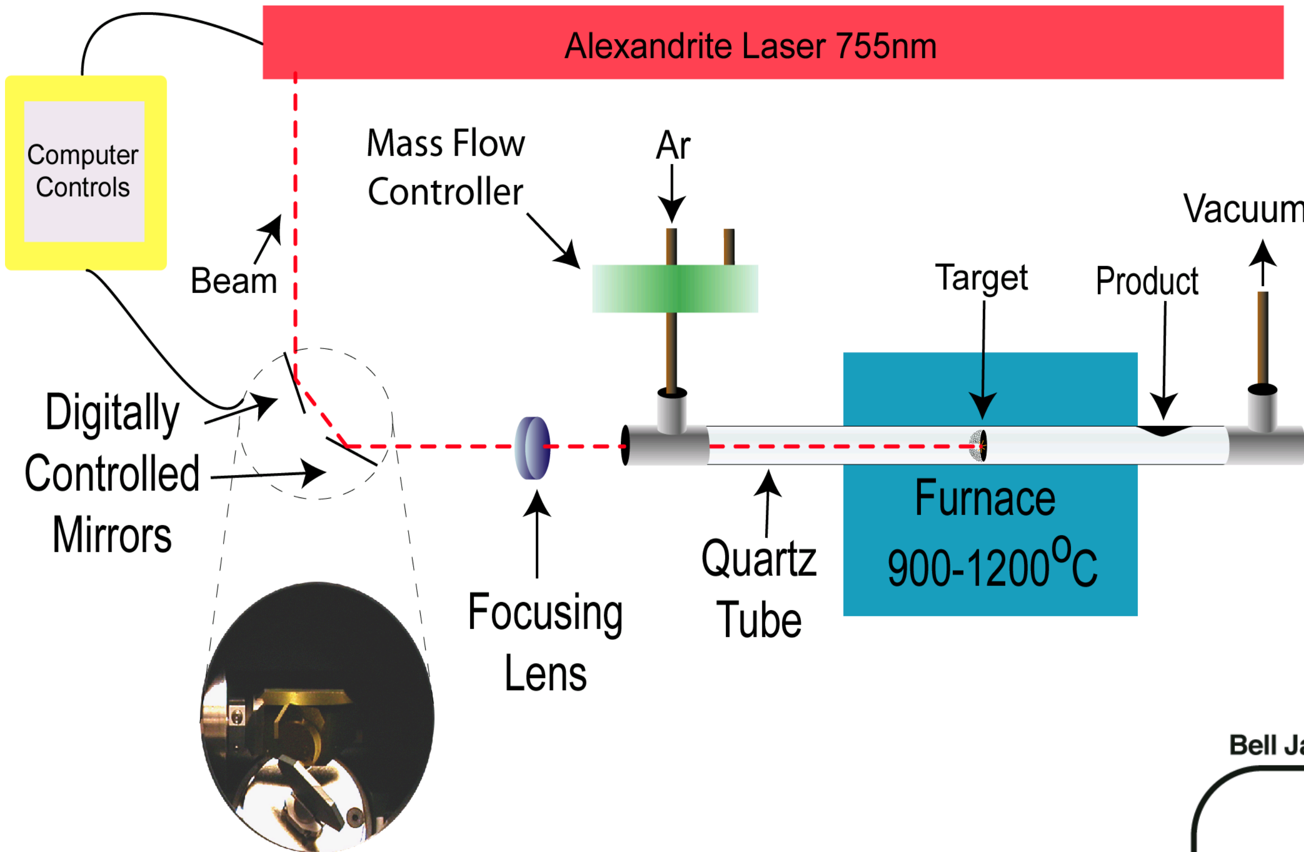

Laser Vaporization
- Highly crystalline and high cost

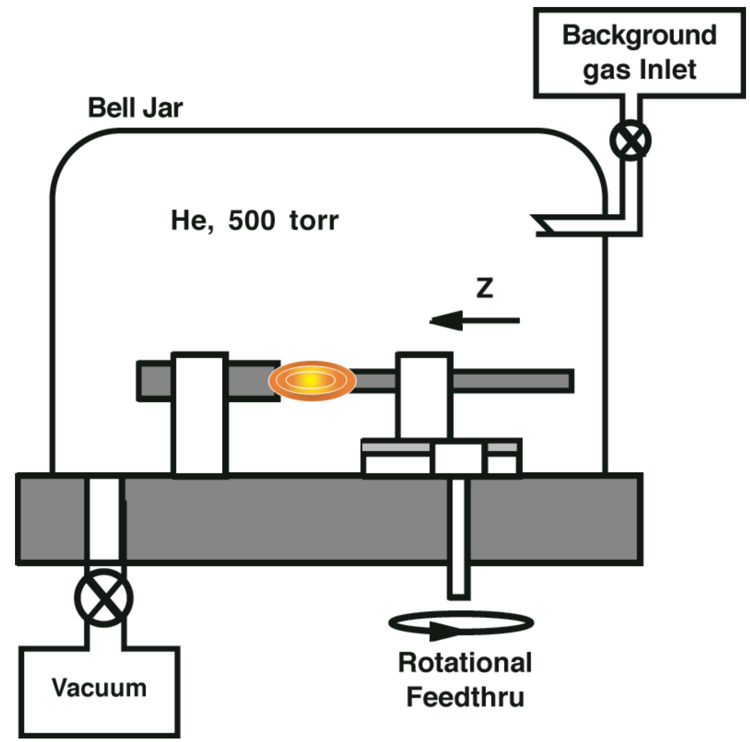

Arc Discharge
- Poorly crystalline and low cost

Arc- vs Laser -generated SWNTs

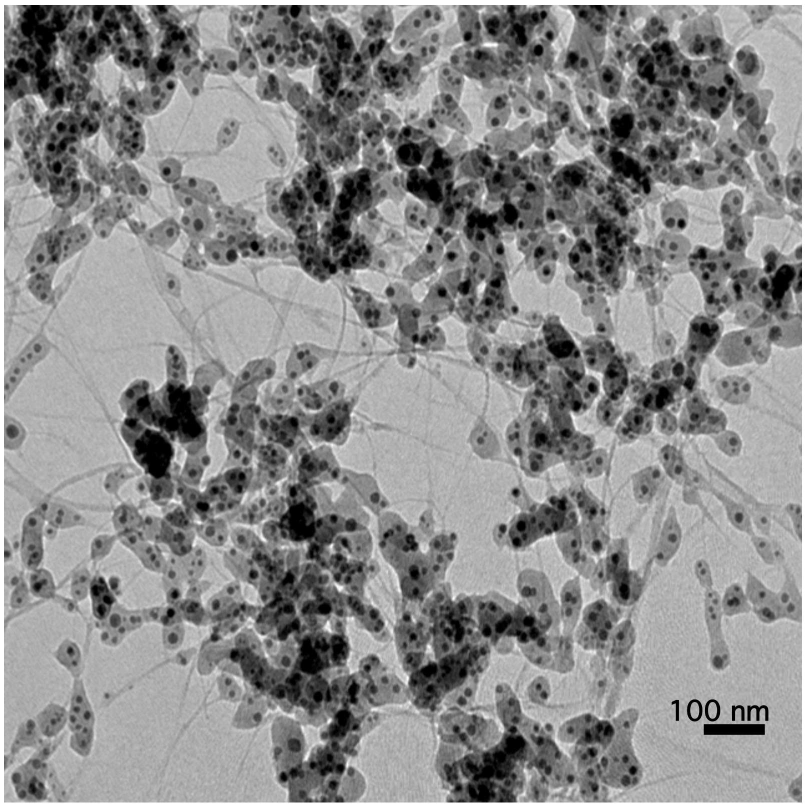

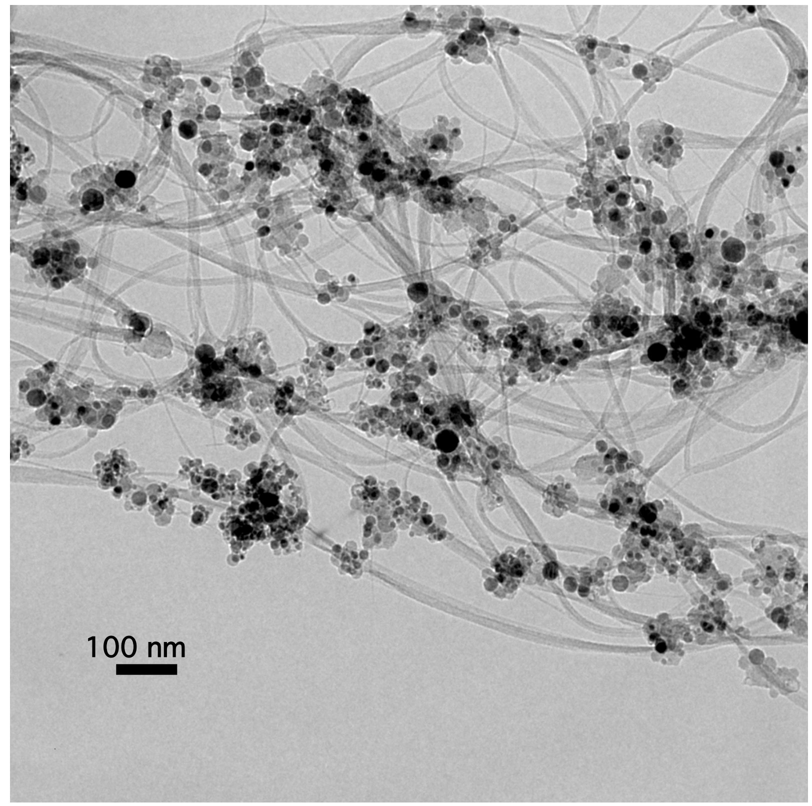

High-Density “Webs” made with Laser Vaporization

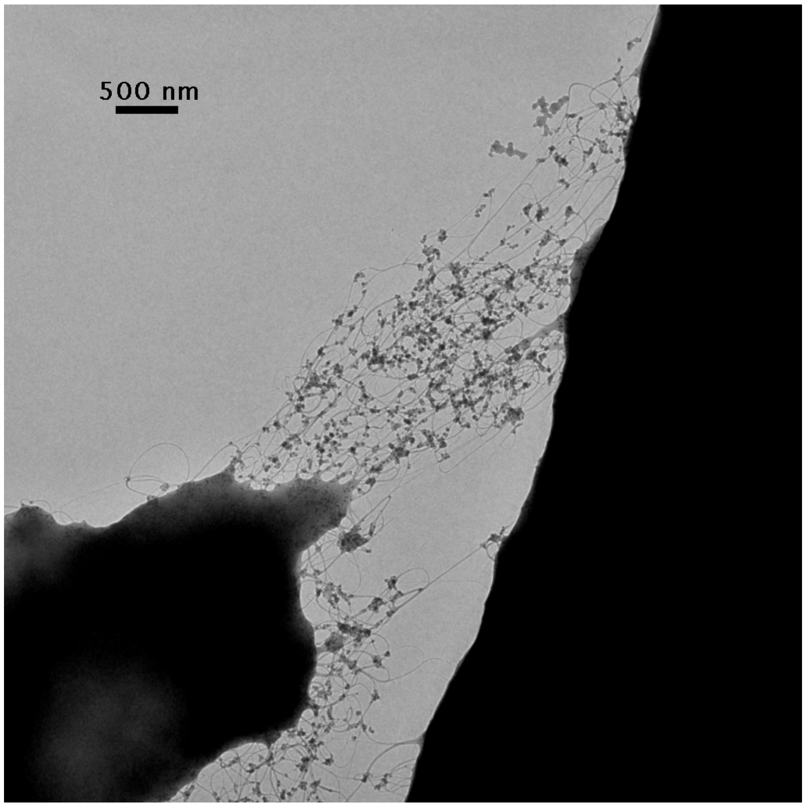

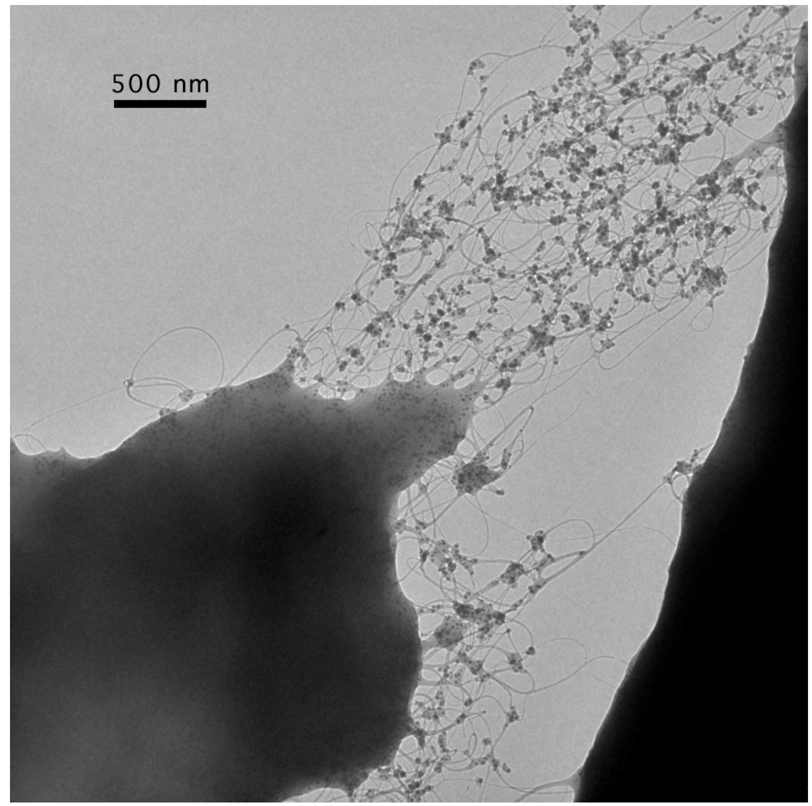

Radial breathing modes

Narrowing the SWNT polydispersity

- during synthesis (laser and chemical vapor growth)
- by selective removal/destruction of specific SWNTs
- chromatography - fractionation by type/diameter

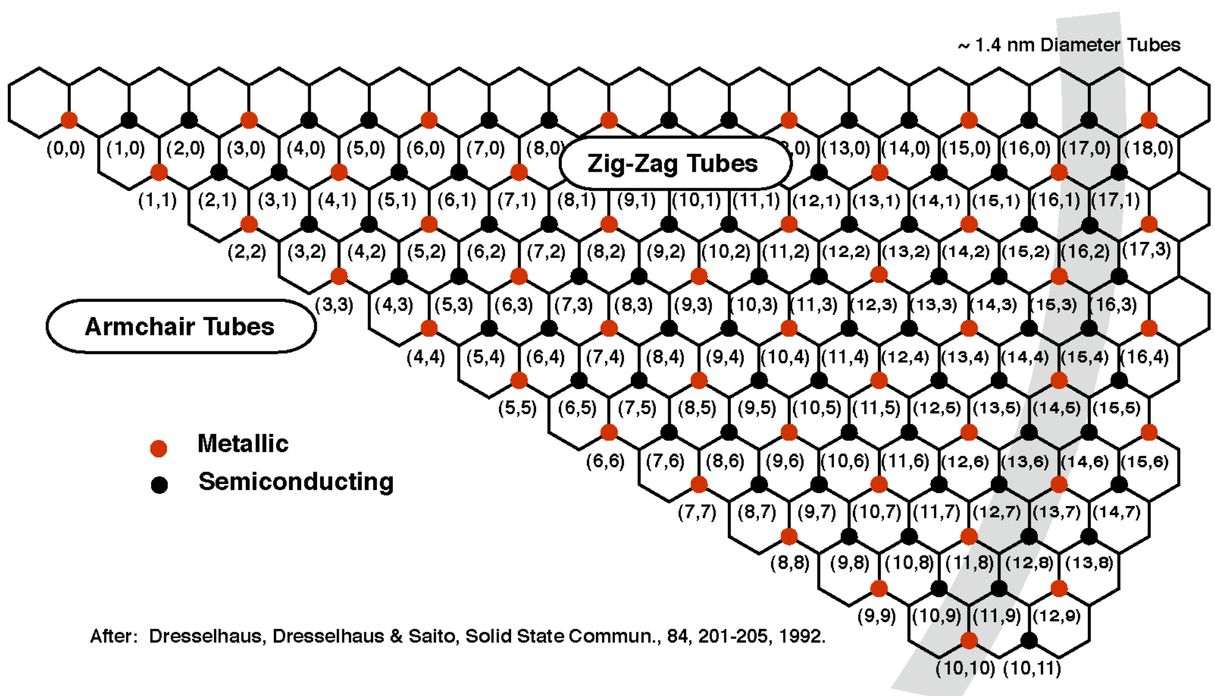

After: Dresselhaus, Dresselhaus & Saito, Solid State Commun., 84, 201-205, 1992.

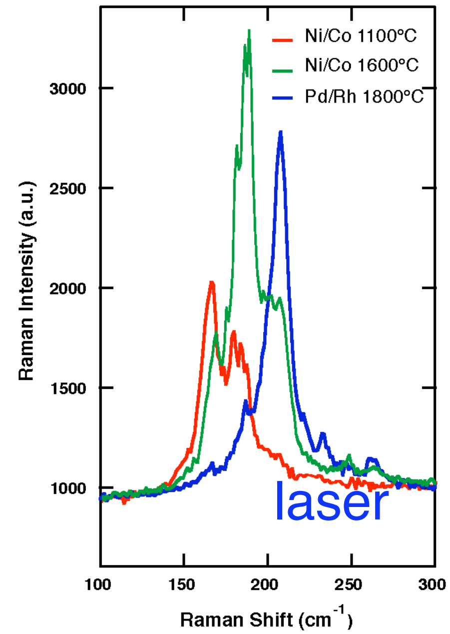

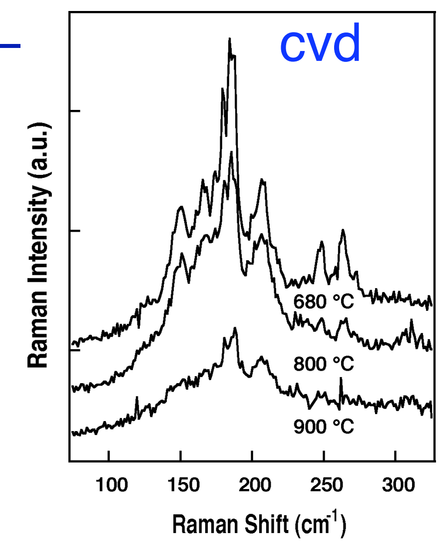

Hornyak, et al., Figure 4

E.g. HiPCO process

Quantitative purification

- Reflux 16 hrs, 3M HNO_3
- 30 min at 500 °C in air
- Final product is highly pure (>98 w%)

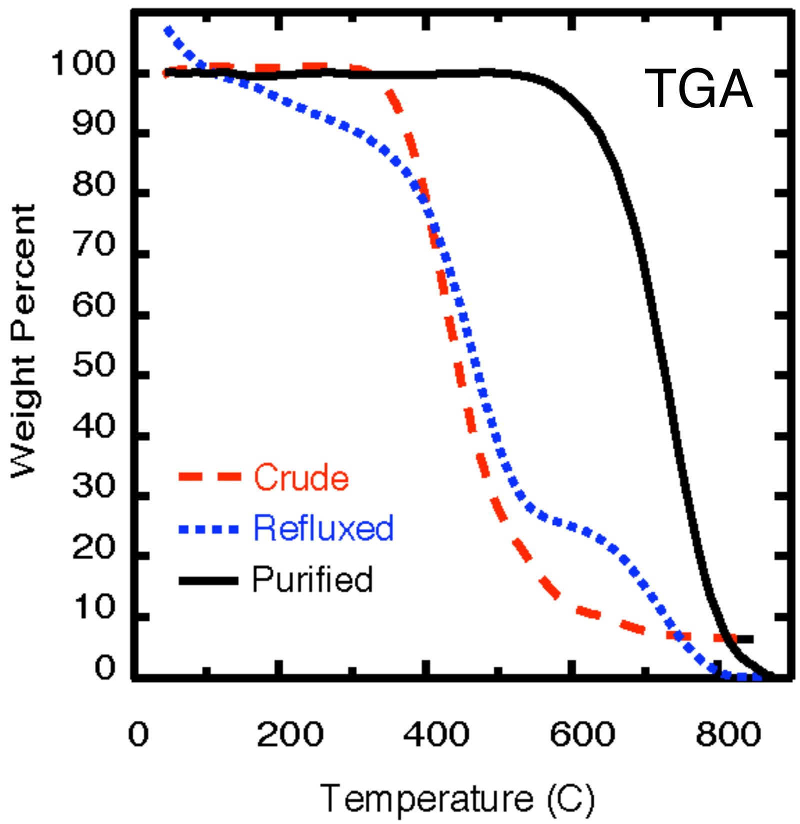

Crude

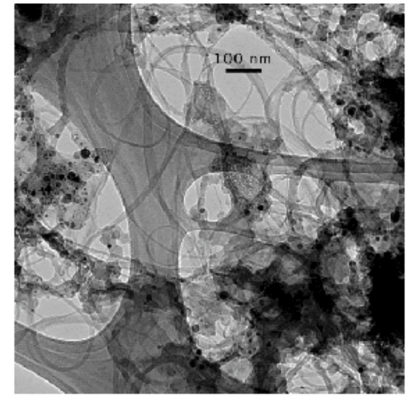

Refluxed

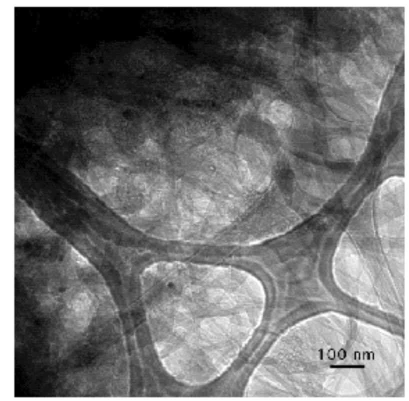

Purified

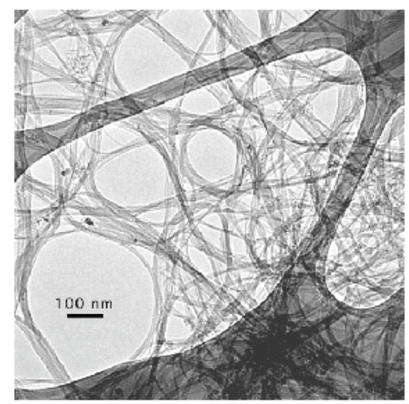

- Goal – scalable, inexpensive, high η solution-processed PV using CNT electrodes as transparent conductors

3D inter-connected networks of CNTs form highly conductive transparent films with good T, R_s

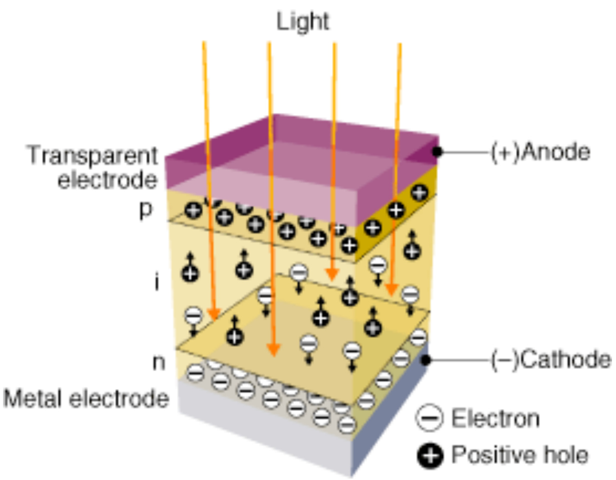

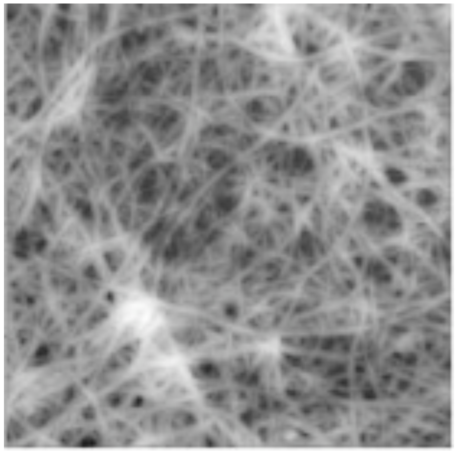

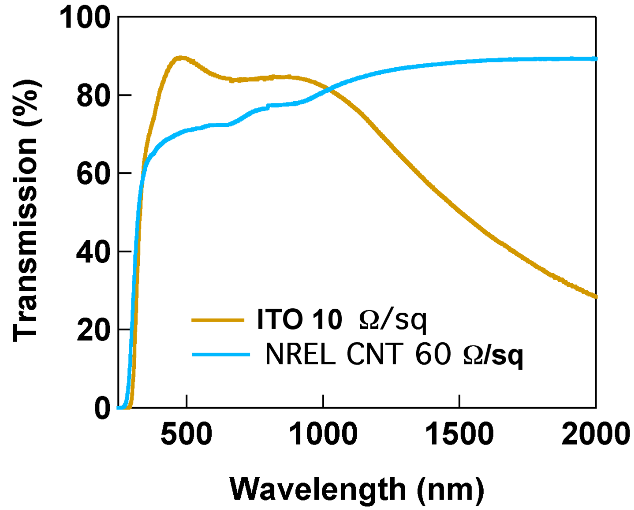

- Thin Film Devices - hope is to achieve high efficiencies at low cost
- Ideally want a fully solution processed cell
- TCOs
  - ZnO:Al, SnO_2:F, In_2O_3:Sn, Cd_2SnO_4

Scalable Production: Ultra-sonic spray

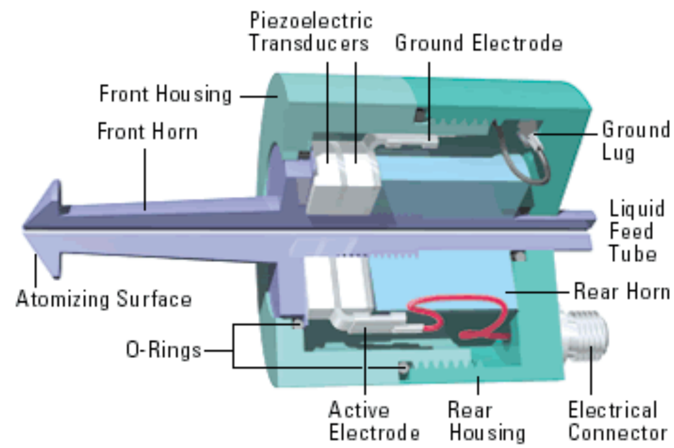

Parameter Matrix:

Purification: metals, non-nanotube C content

Surfactant: SWCNT dispersion, bundle size

Surface Functionalization: wetting, drop formation

Sonication: SWCNT length, bundle size, defects

Post Process Treatments: surfactant removal, doping

Metrics: transparency, conductivity, stability

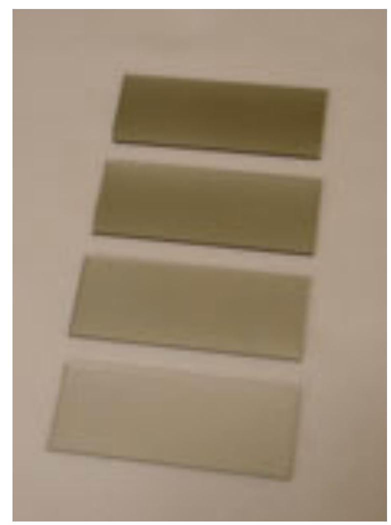

1 x 4 inch

What Makes a Good SWNT Electrode?

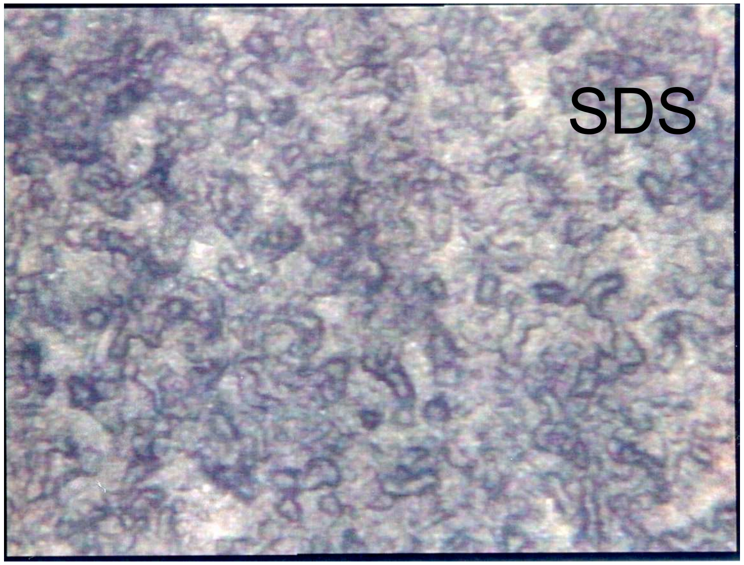

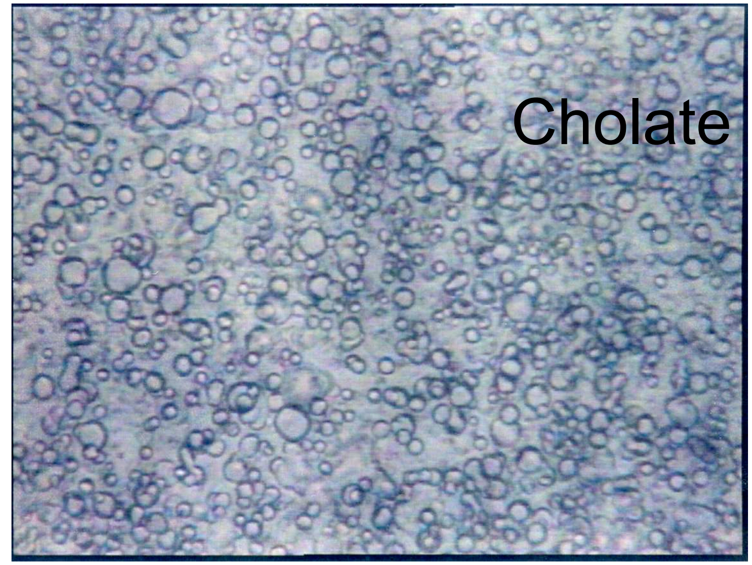

Surfactants & Macro-morphology

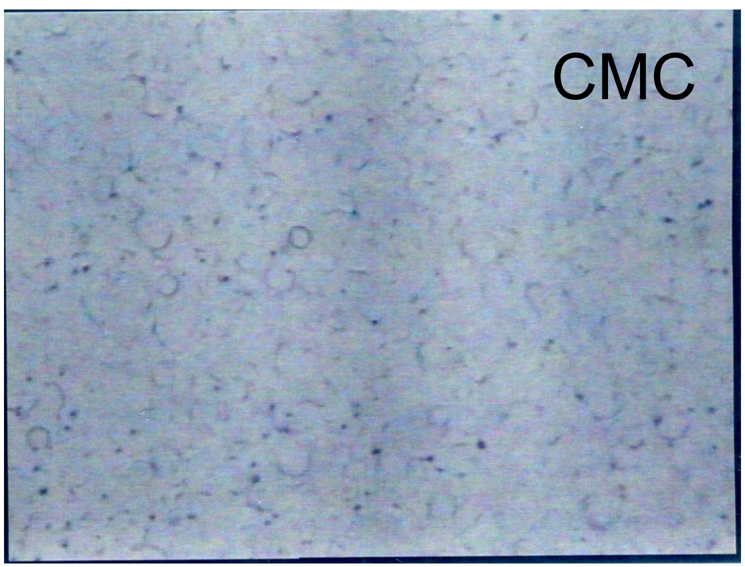

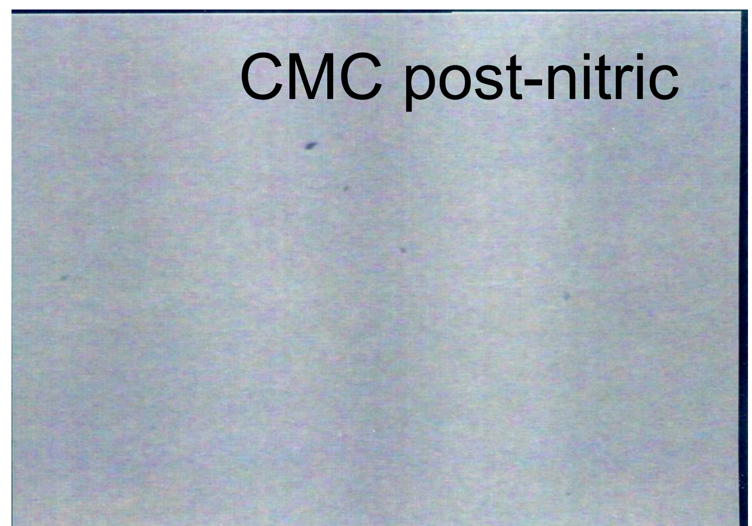

Tenent et al., Adv. Mater. 2009, 21, 1–7

Processing of Sprayed CMC Films

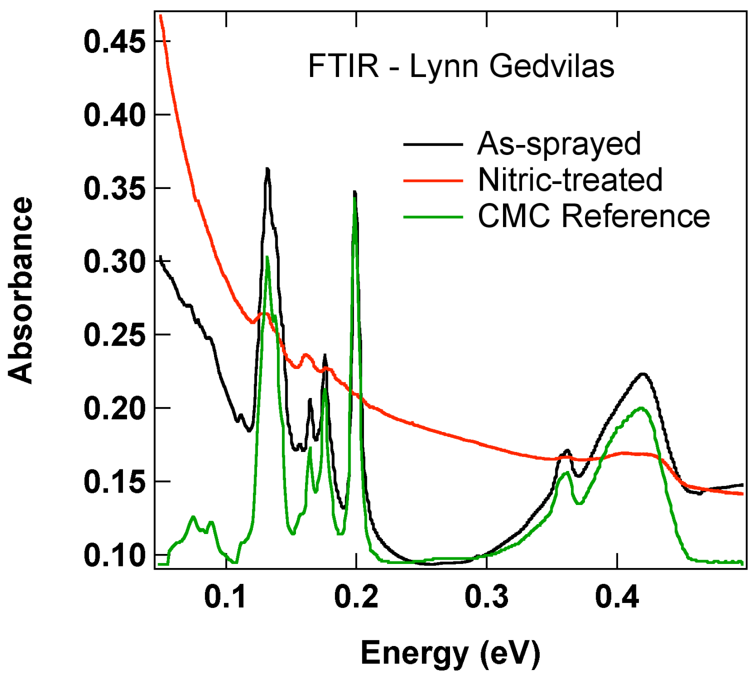

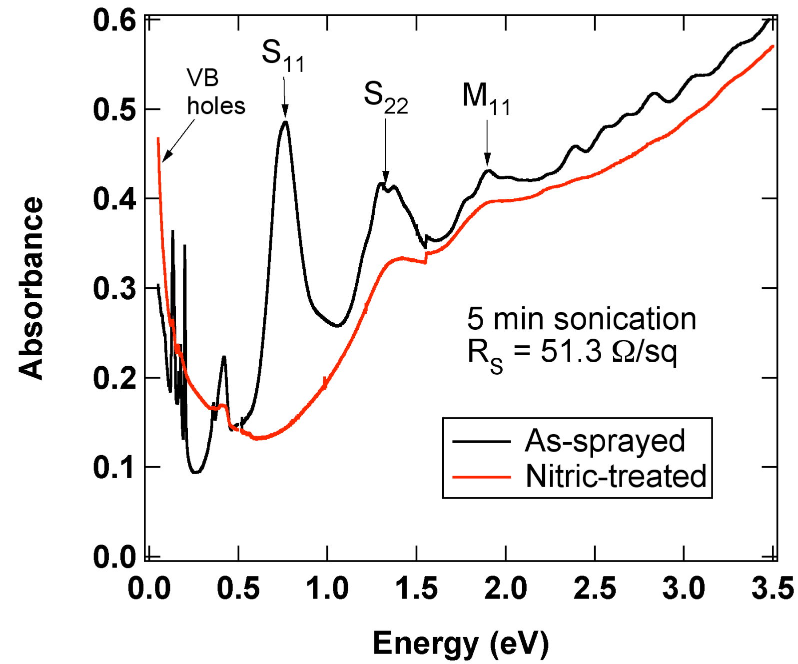

Profilometry:

As-sprayed = 614 +/- 16 nm

Post-nitric = 43 +/- 5 nm

- FTIR confirms removal of CMC
- profilometry confirms densification of network
- Several likely oxygen related peaks still present, but greatly attenuated
- SWNT interband transitions bleached by HNO_3
- "free carrier plasma" in IR after HNO_3 due to intraband hole transitions

Tenent et al., Adv. Mater. 2009, 21, 1–7

What Makes a Good SWNT Electrode? Continued

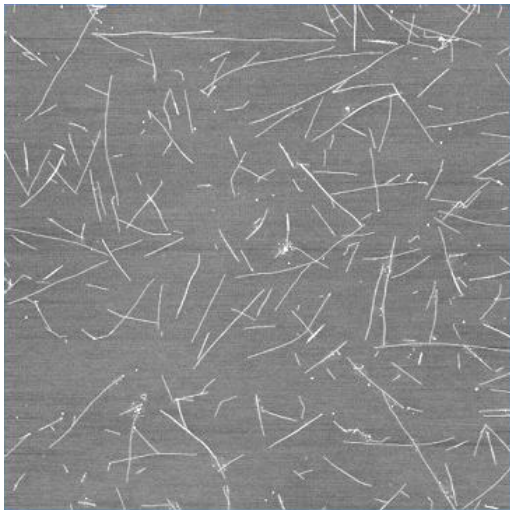

10 minutes

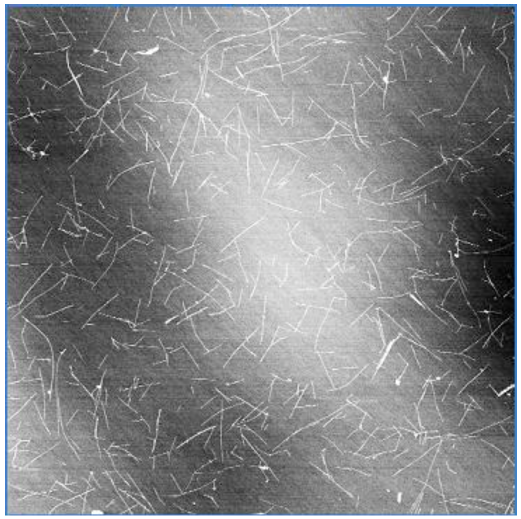

60 minutes

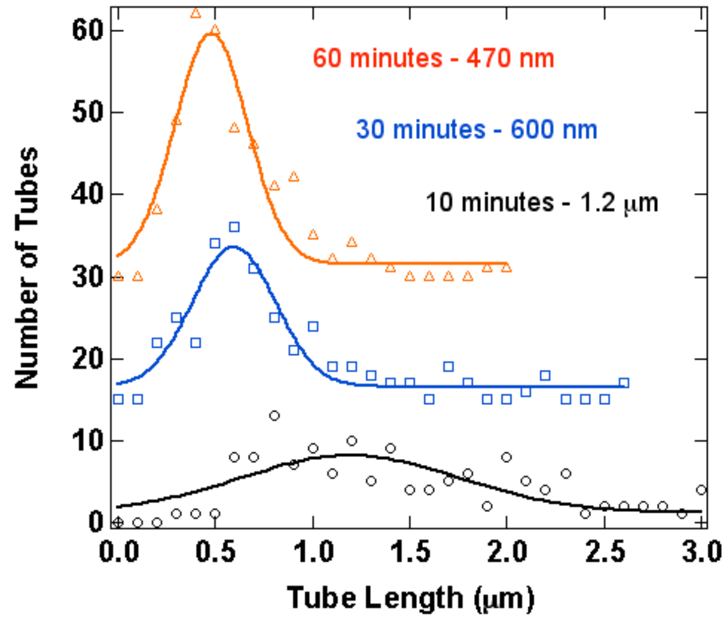

Sonication Time and Tube Length

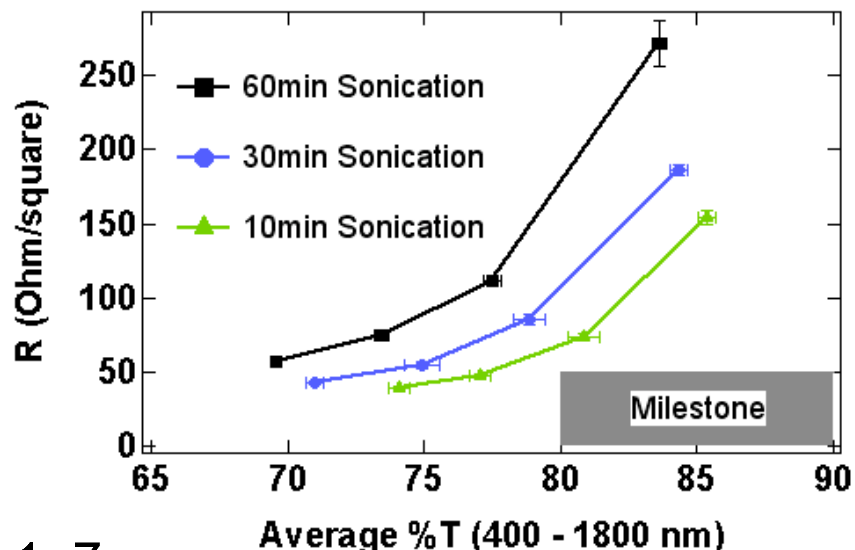

Tenent et al., Adv. Mater. 2009, 21, 1–7

OPV Device Structures -sprayed SWNT Electrodes

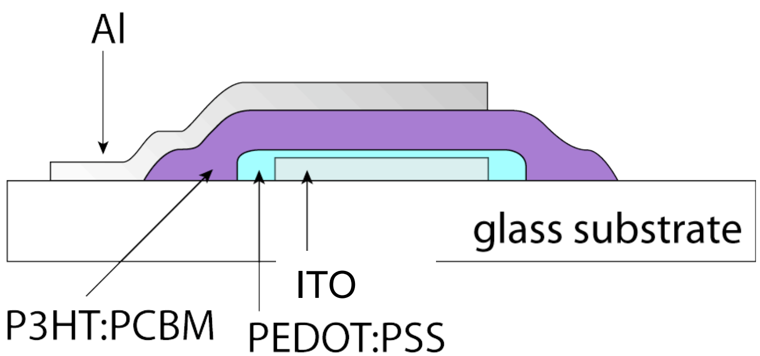

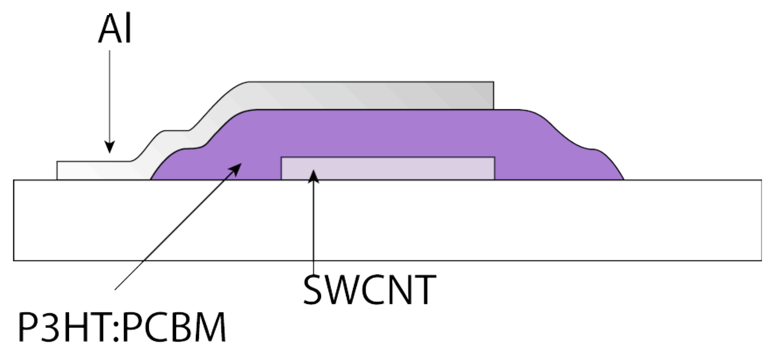

Mix P3HT and PCBM in a 1:1 ration to create a bulk heterojunction

P3HT carries holes to the ITO side, PCBM transports electrons to Al

Early OPV Device Results: collaboration with Eikos

J. van de Lagemaat, T. M. Barnes, G. Rumbles et al., Applied Physics Letters **88** (23), 3 (2006).

Devices on NREL SWCNT Networks

-Ultrasonic spray deposition
-Several ~ 3% devices
-Thick active layers - spun at 200 rpm
-Reducing electrode roughness is key
-PEDOT can be eliminated

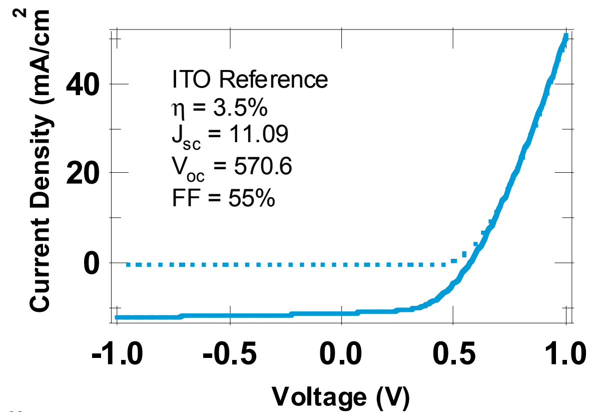

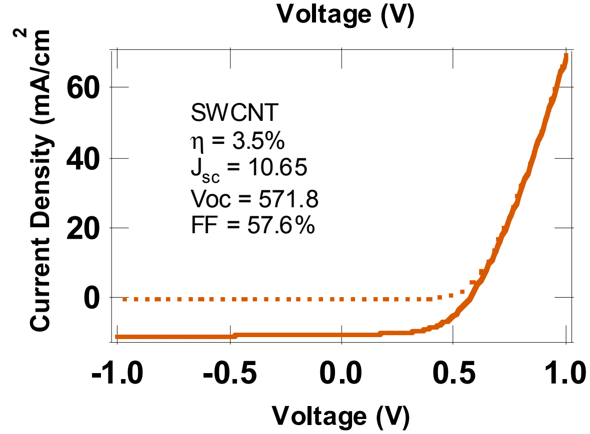

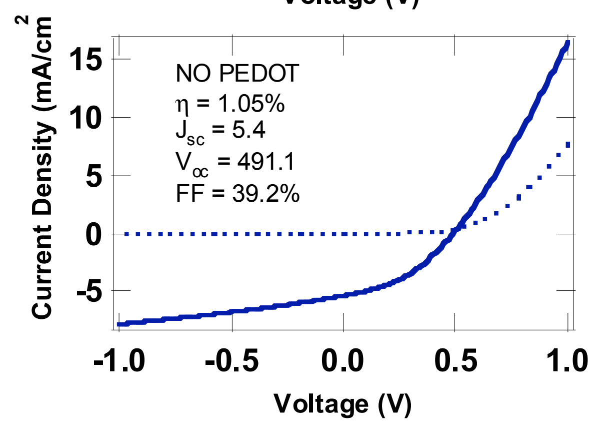

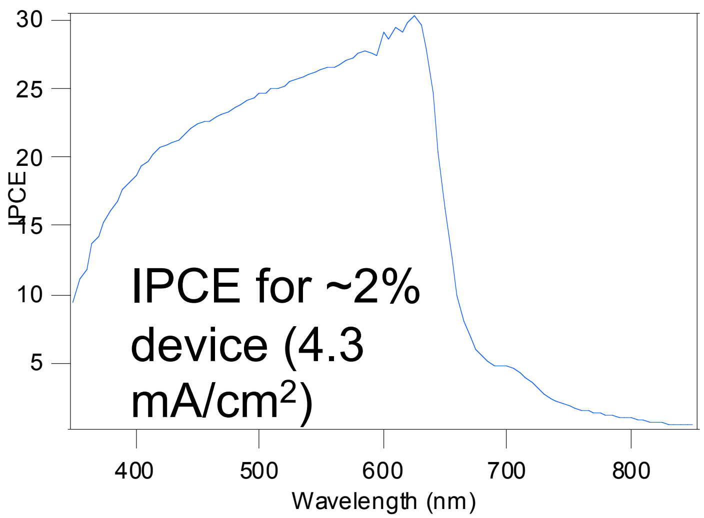

Exciton dissociation and charge collection in a C_{60} – SWNT PV device

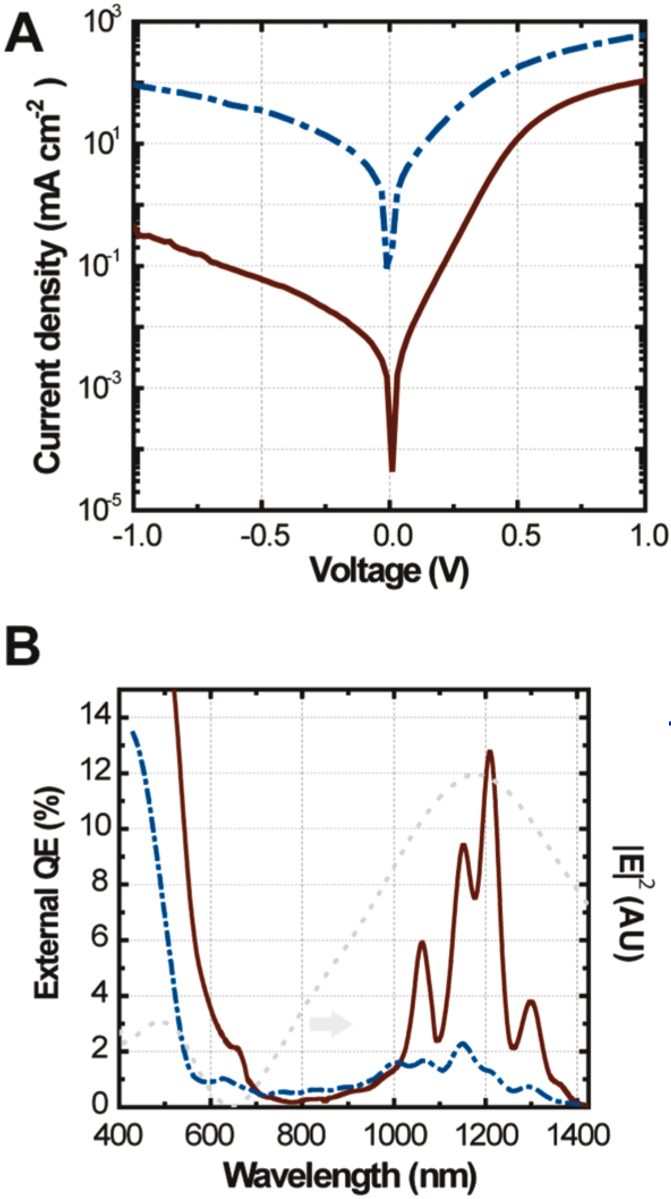

Comparison of characteristics of mixed-SWCNT (dot-dash, blue) and semi-SWCNT (solid, red) devices.

(A) Typical dark current-voltage characteristics. (B) Spectrally resolved short-circuit external QE for devices with optimized thicknesses, and spectrally varying optical intensity at the s-SWCNT/C60 interface (gray, dashed) predicted using optical transfer matrix simulations.

“*Efficiently Harvesting Excitons from Electronic Type-Controlled Semiconducting Carbon Nanotube Films*”, Michael S. Arnold et al., dx.doi.org/10.1021/nl1031343 | Nano Lett. 2011, 11, 455–460.

Exciton dissociation and charge collection in a C_{60} – SWNT PV device

Photovoltaic and photodetector response.

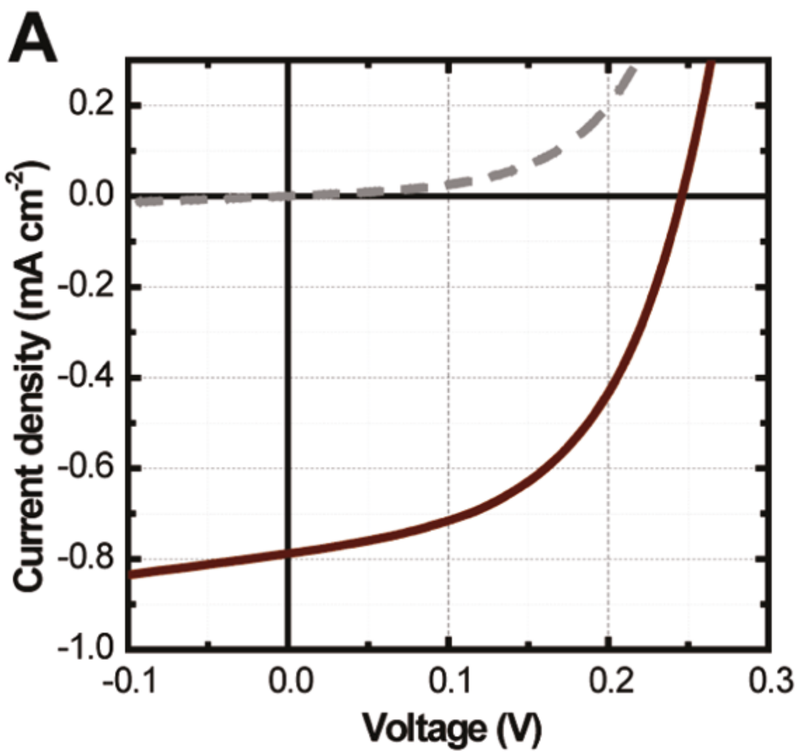

Current-voltage characteristics in the dark (dashed, gray) and in response to 17 mW cm^{-2} NIR (1000-1365 nm) illumination (solid, red).

"*Efficiently Harvesting Excitons from Electronic Type-Controlled Semiconducting Carbon Nanotube Films*", Michael S. Arnold et al., dx.doi.org/10.1021/nl1031343 | Nano Lett. 2011, 11, 455–460.

SWNTs are Tunable Extended Molecules

(n,m) indices

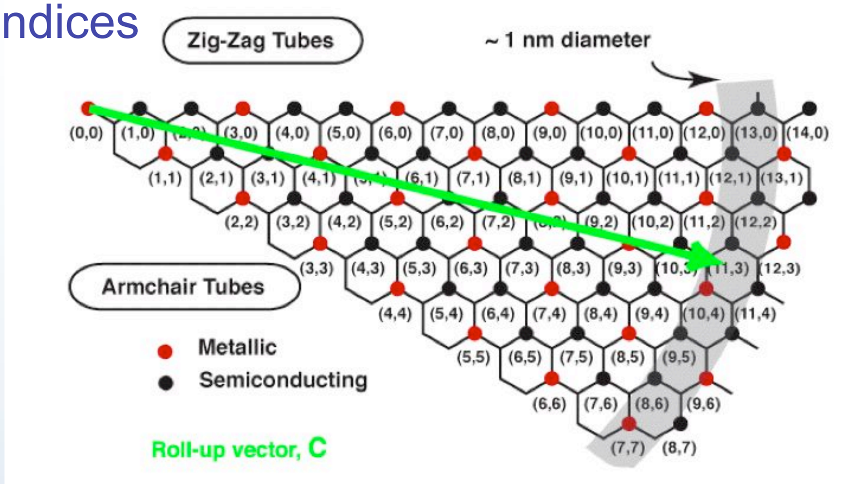

After: Dresselhaus, Dresselhaus & Saito, Solid State Commun., 84, 201 (1992)

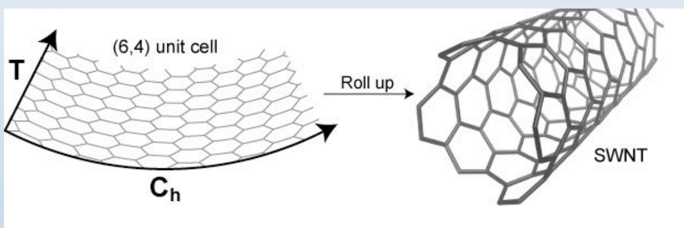

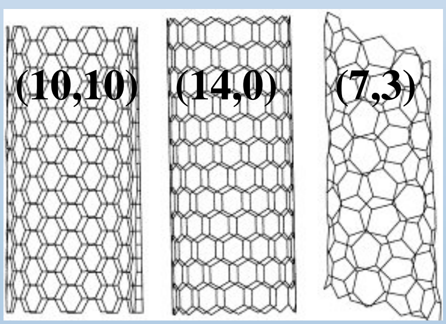

armchair zigzag chiral

Dodziuk et al. *CPL* 356 (2002) 79

Van Hove singularities

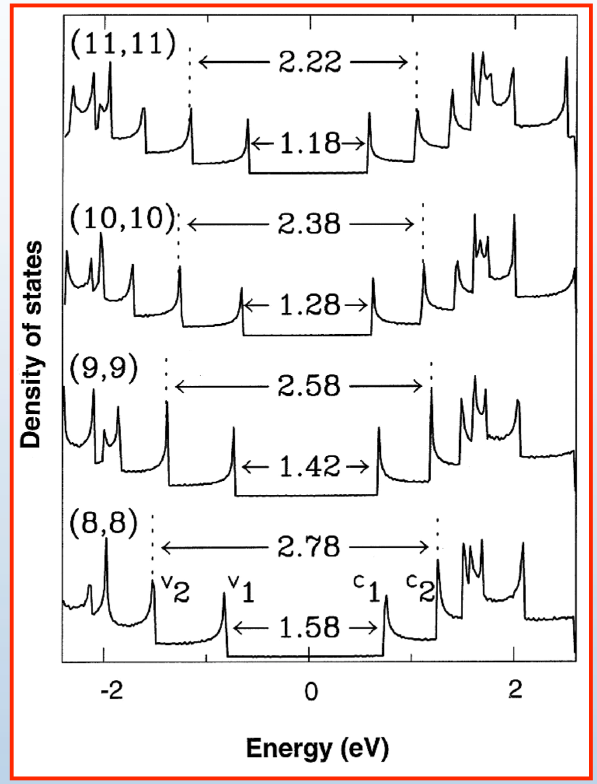

Rao et al., *Science* 257, 187 (1997)

*Metallic when n-m = 3 * I*
All others are semiconductors

Nanotubes in Solar Energy Convertors

Hole-collecting SWNTs

Du Pasquier et al., APL **2005**, 87, 203511

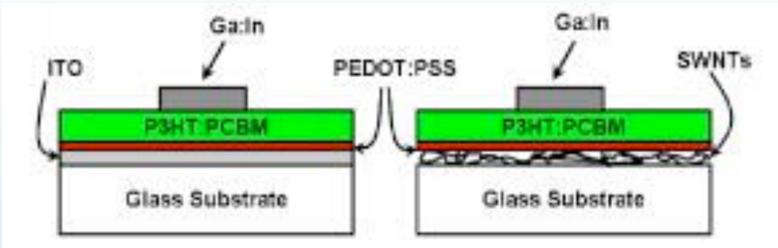

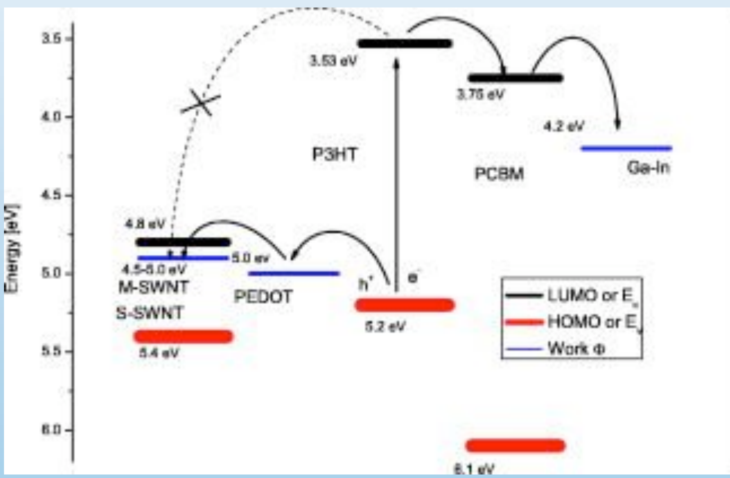

1% efficiency vs. 0.65% with SWNTs (AM 1.5)

Electron-collecting SWNTs

Guldi et al., *ACR* **2005**, 38, 871

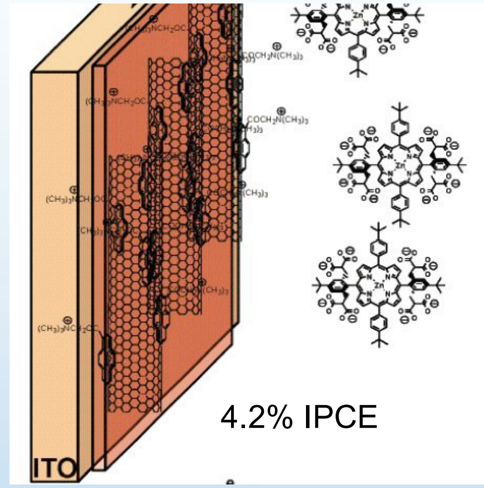

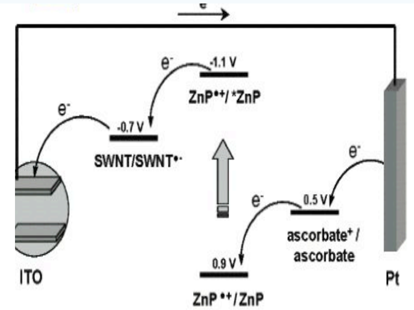

Hasobe et al., JPCB **2006,** 110, 25477

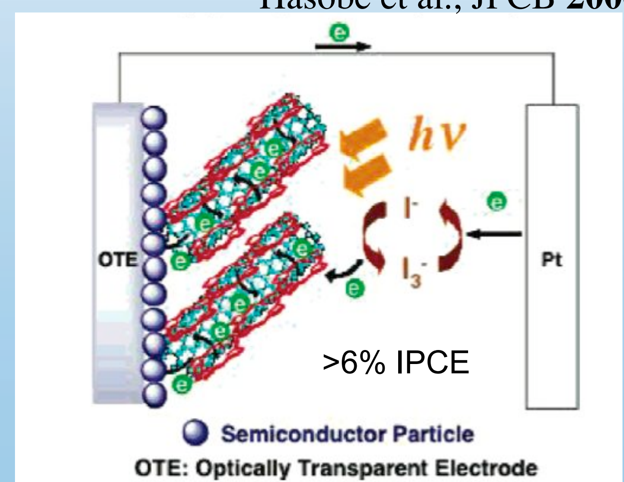

SWNTs as Solar Absorbers?

- Good Overlap with Solar Spectrum

R. Saito et al., PRB 61, 2981 (2000)

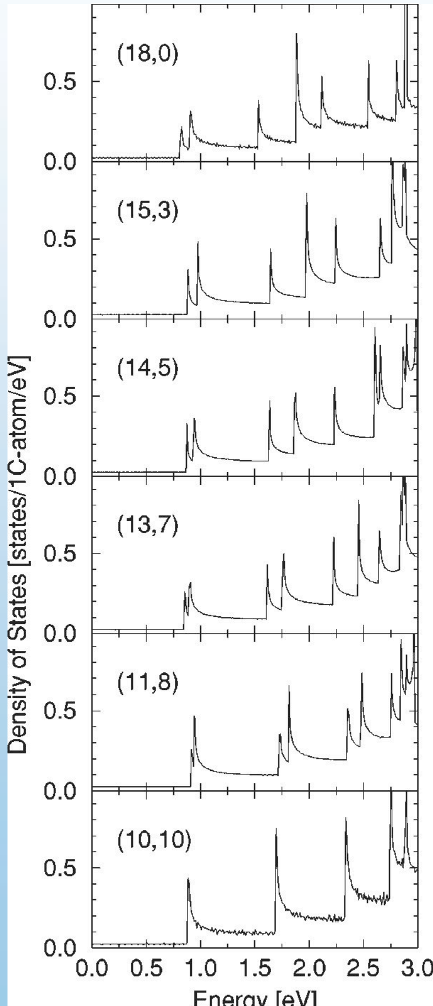

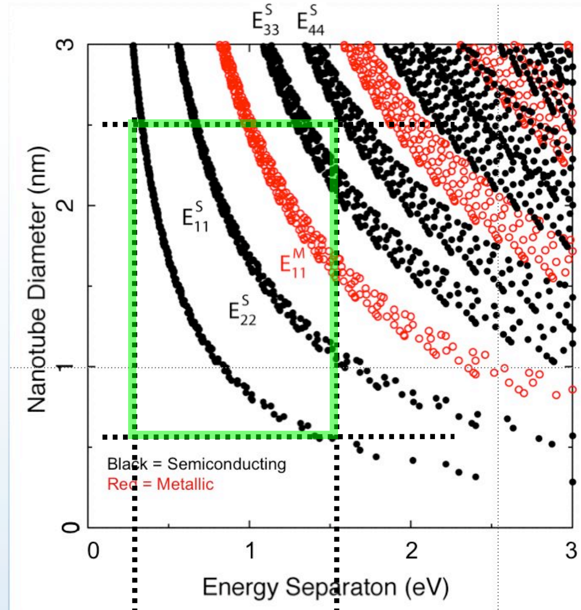

Kataura Plot
(S. Maruyama, http://www.photon.t.u tokyo.ac.jp/~maruya ma/kataura/kataura.h tml)

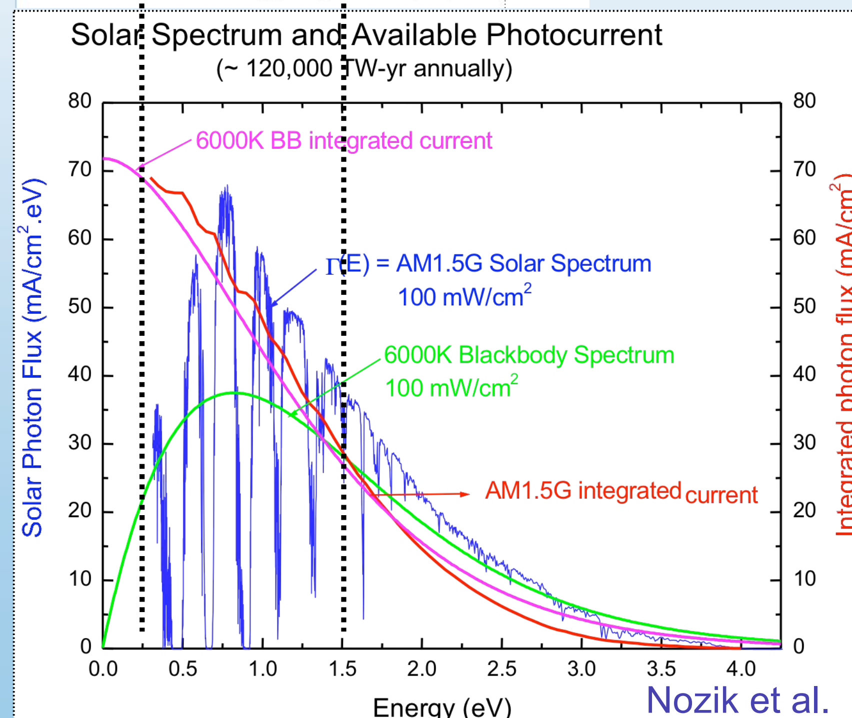

Topics / Outline

(1) What limits QY of SWNT PL?

(2) Absolute potentials of SWNT HOMO and LUMO.

(3) Towards type-pure solar conversion architectures.

Solubilizing SWNTs with Surfactants

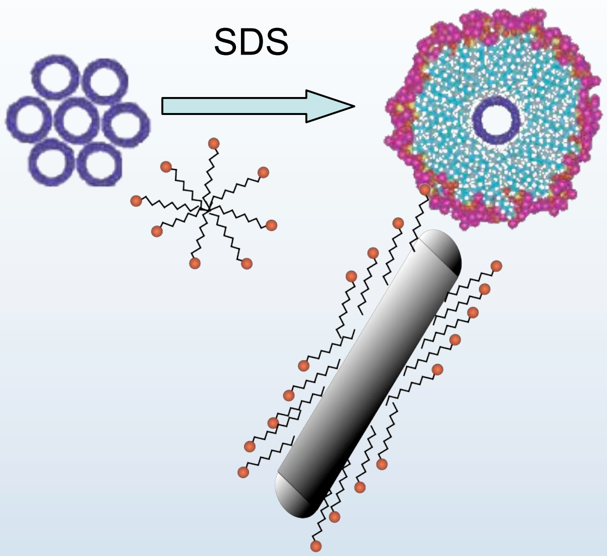

Structured UV-Vis

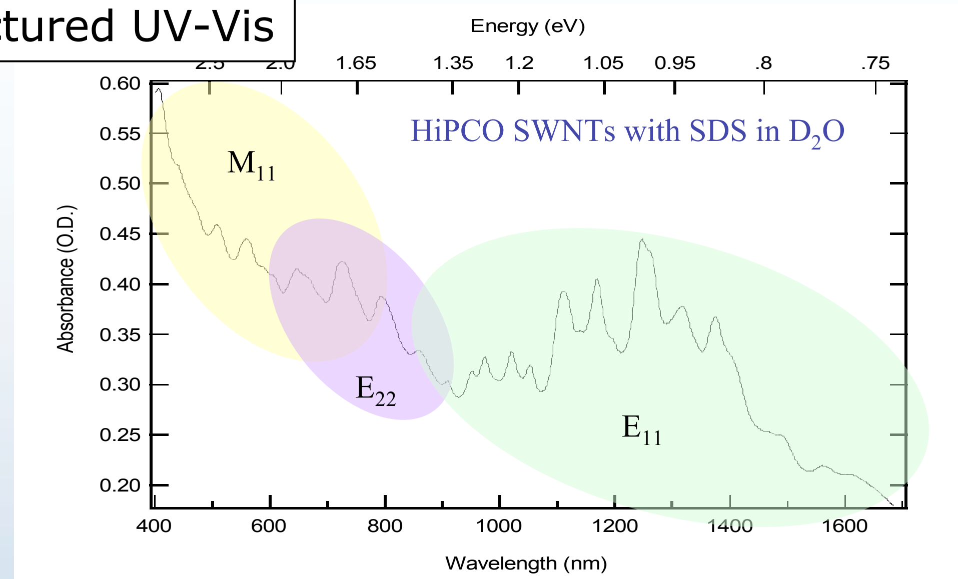

B-doped[1]

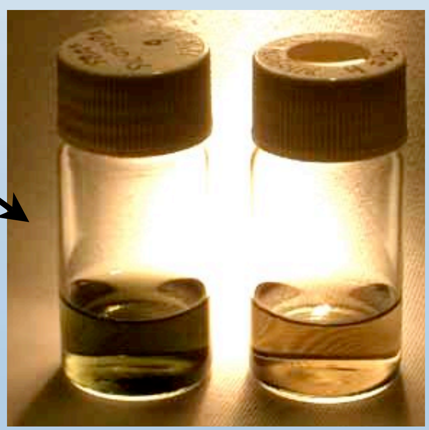

Pure C

Photoluminescence[2]

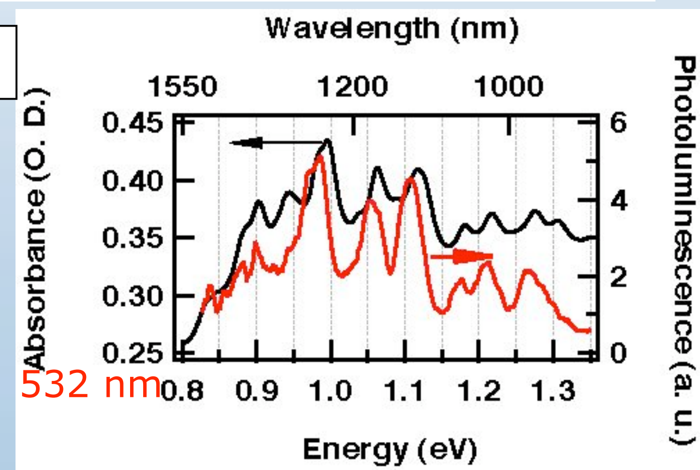

[1]Blackburn et al. *Chem. Mat.* **2006**, 18, 2558

[2]O'Connell et al., *Science* **2002**, 297 593

PL Landscape

Fast FT-PL spectrometer[1] probes all known nanotube species

SDS

HiPco (cvd)

Pulsed laser vaporization (homemade)

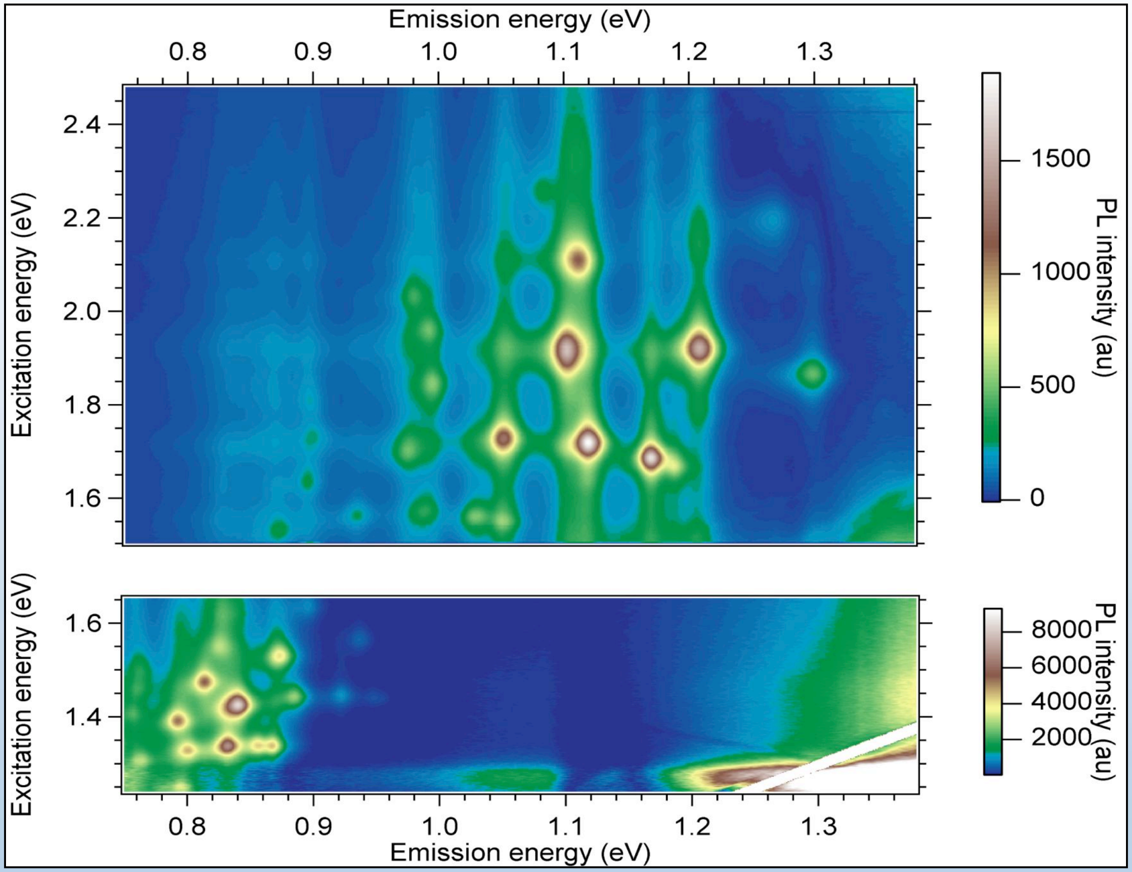

~ 20 luminescent species

Metallic tubes not seen

~ 20 luminescent species

PL from tubes with diameters from 0.76 nm to 1.4 nm

[1] *McDonald et al., Rev. Sci. Inst.* **2006**, *77*, 053104

Photoexcitation Relaxation Dynamics

Potential to do chemistry or generate a photovoltage in a device with photoexcited SWNTs depends on the competition between relaxation mechanisms

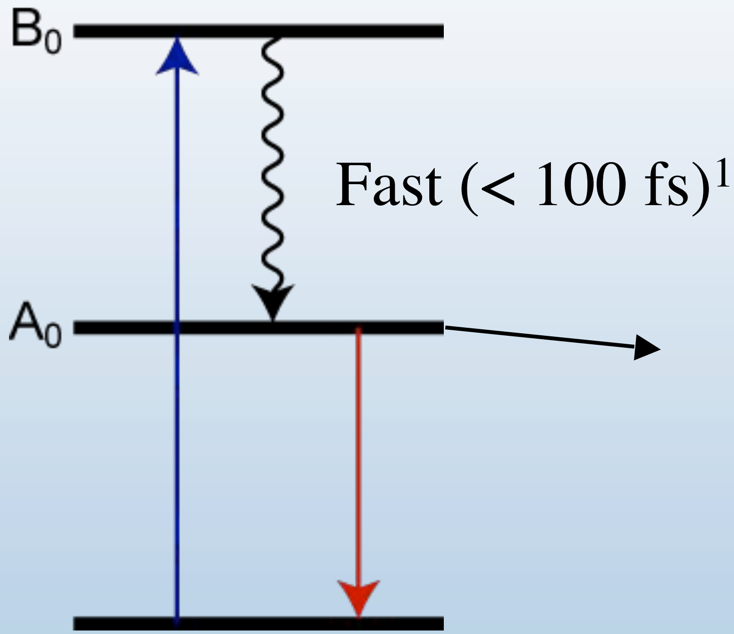

[1]Ma et al. *J. Chem. Phys.* **2004**, 120, 3368

Photoexcitation Relaxation Dynamics

Fluorescence lifetimes:

<10 ps: Fluorescence upconversion - Ma et al. *JCP* **120** (2004),
15 ps: TCSPC - Hagen et al., *APA* **78** (2004).
7 ps: Kerr gating - Wang et al., *PRL* 92 (2004).
120 ps: TCSPC - Jones et al., *PRB* **71** (2005).

Low quantum yields for ensembles: ($\Phi \sim 10^{-3} - 10^{-4}$)

$$1/\tau_{PL} = 1/\tau_{NR} + 1/\tau_{R}$$

$$\Phi = \tau_{PL} / \tau_{R}$$

$$\tau_{PL} \sim \tau_{NR} << \tau_{R}$$

Experimental determination of τ_R

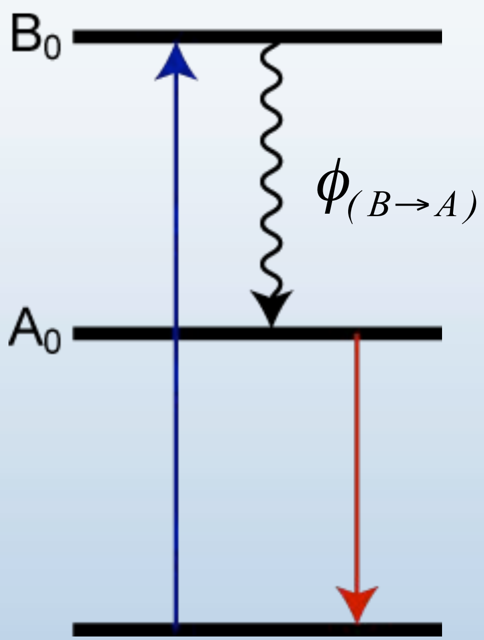

$$\eta_{PL} = \frac{k_R}{k_R + k_{NR}} = \frac{\tau_{PL}}{\tau_R}$$

$$\begin{bmatrix} \tau_{PL} = 130\,ps \\ \eta_{PL}^{lit} = 10^{-3} \end{bmatrix} \Rightarrow \tau_R = 130\,ns$$

…a factor of 4 - 40 too long in comparison to theory[1]

measured η could be low:

- absorption by metal tubes
- PL quenching by tube-tube interactions
- extrinsic factors

[1]Perebeinos, et al., Nano Letters 5, 2495-2499 (2005)

“Extrinsic factors” in Time-resolved PL Studies

General consensus:
PL lifetimes limited by extrinsic effects; i.e. *defects, kinks, ends, environmental factors*

PL for different, single (6,4) tubes - 87 K

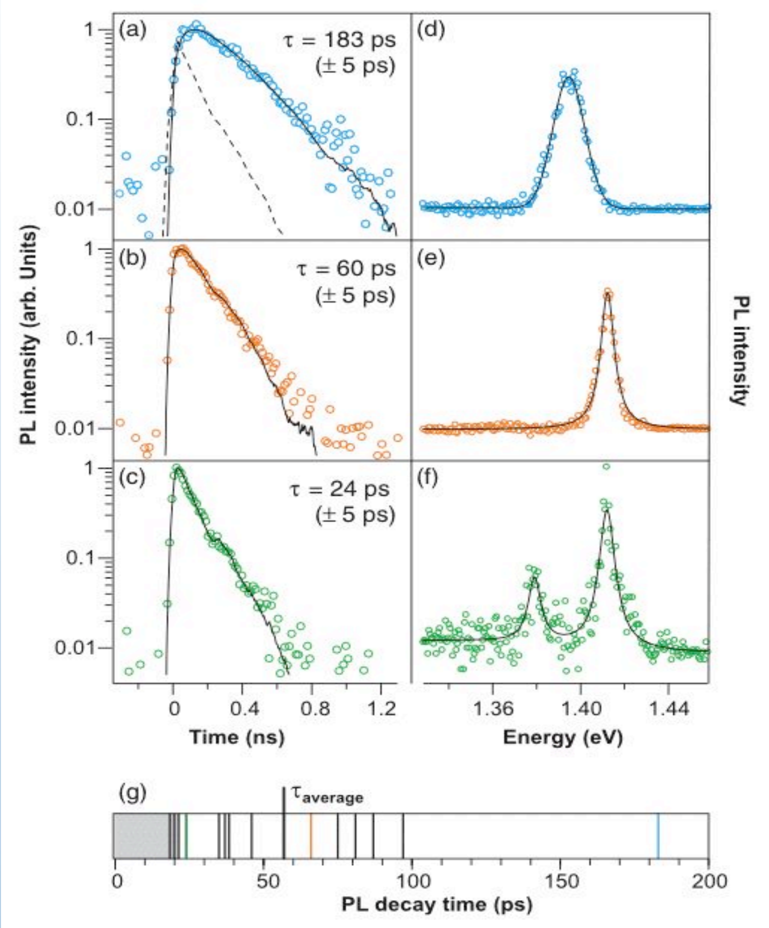

Hagen, et al., PRL 95 (2005).

NREL National Renewable Energy Laboratory

Past and Recent PL QY Reports

Report	Synthesis	Surfactant	ϕ_{PL} (%)
1. O'Connell	Raw HipCo	SDS	~0.1
2. Wang	Raw HipCo	SDS	~0.017
3. Jones	Raw HipCo	SDS	~0.05-0.65
4. Lefebvre	CVD	none	~7
5. Krauss	CoMoCat	cholate	~2
6. Weismann	Raw HipCo	SDS	1 – 8

Rows 1–3: ensembles

Rows 4–6: single tubes

1. Science, **297**, 593 (2002)
2. P.R.L., **92**, 177401 (2004)
3. P.R.B., **72**, 115426 (2005)
4. Nano Lett., **6**, 1603 (2006)
5. Abstracts of March 2007 APS D.28.8
6. Abstracts of April 2007 MRS EE4.3

Enhanced PL for "*un-purified*" Samples

Acid-purified SWNTs in Sodium Cholate (SC)

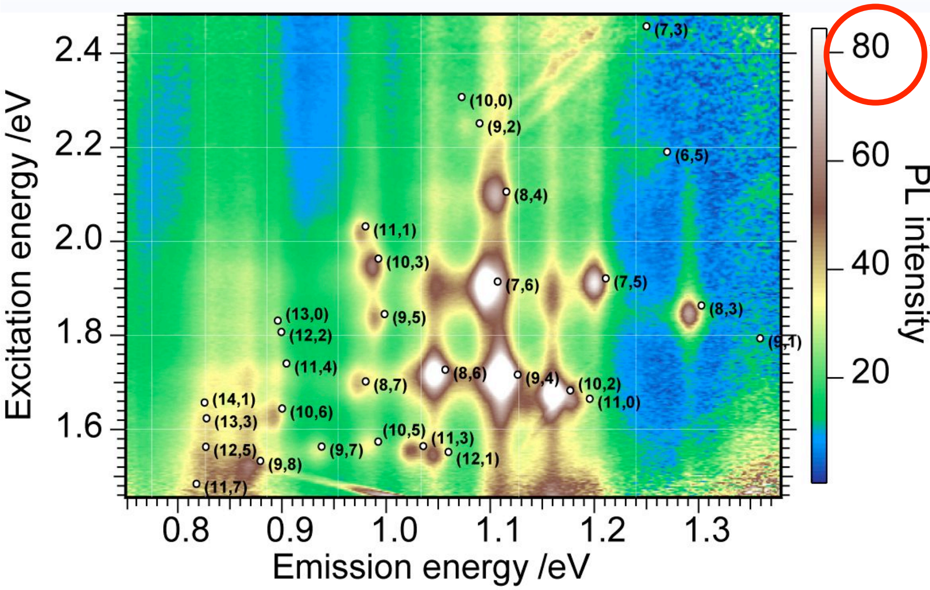

Raw SWNTs in SC

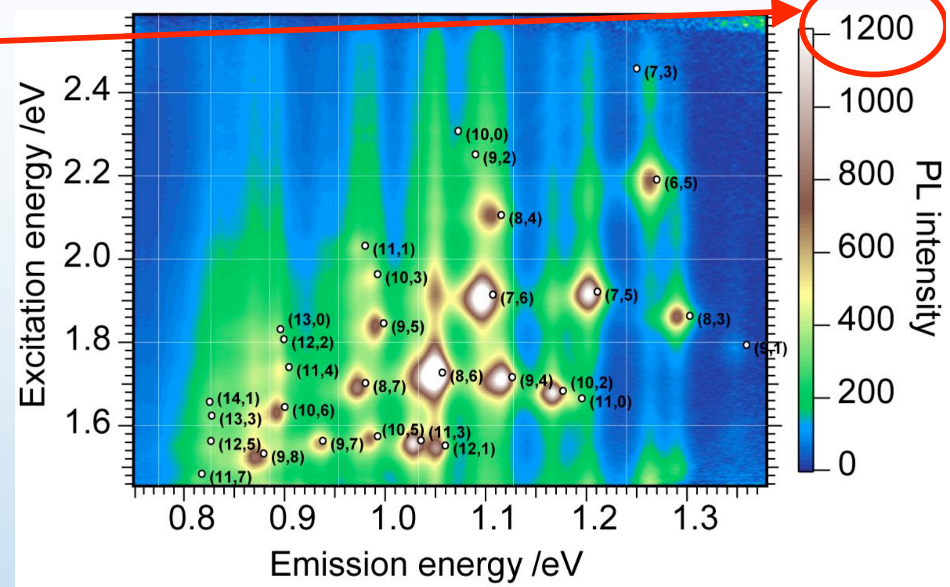

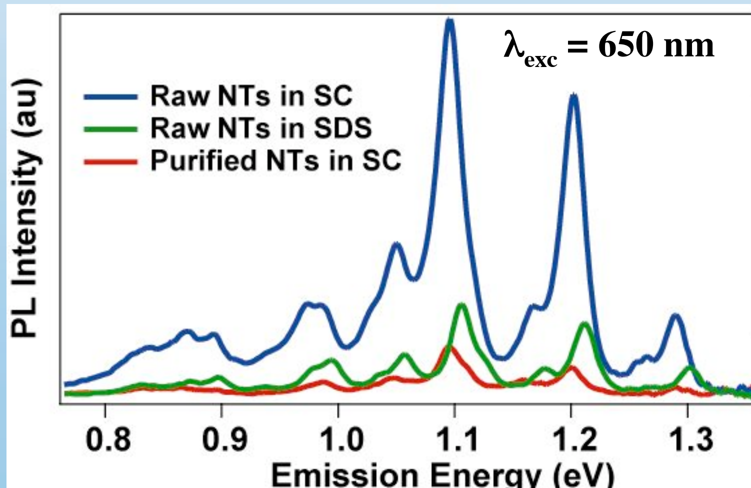

Greater than 4 % for Several (n,m) Species

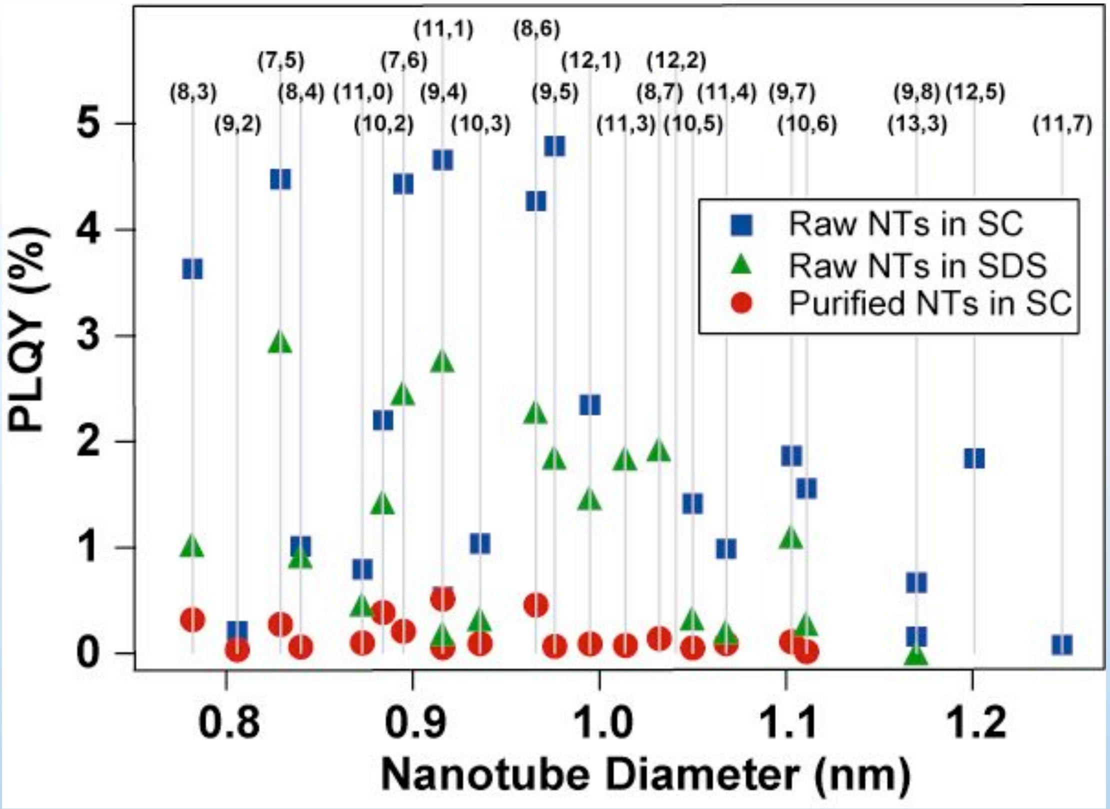

- **Measured relative to IR26 (ϕ_{PL} = 5 x 10^{-3}) in DCE**
- **Highest reported values for ensemble SWNT dispersion**
- **Catalytic synthetic metal particles still present…**

Why?

Samples exposed to acids remain protonated (hole-doped)

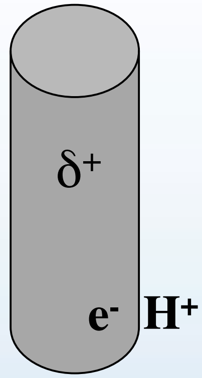

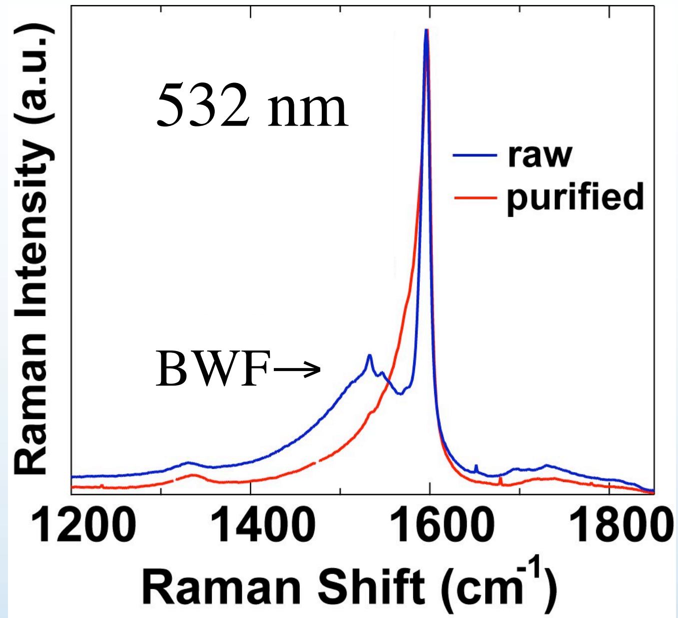

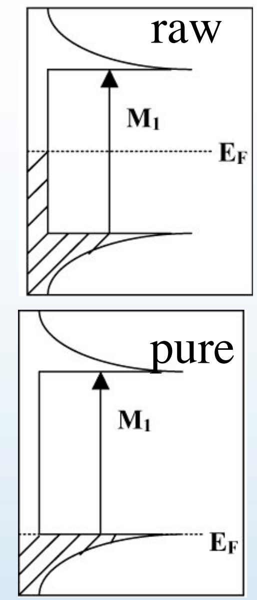

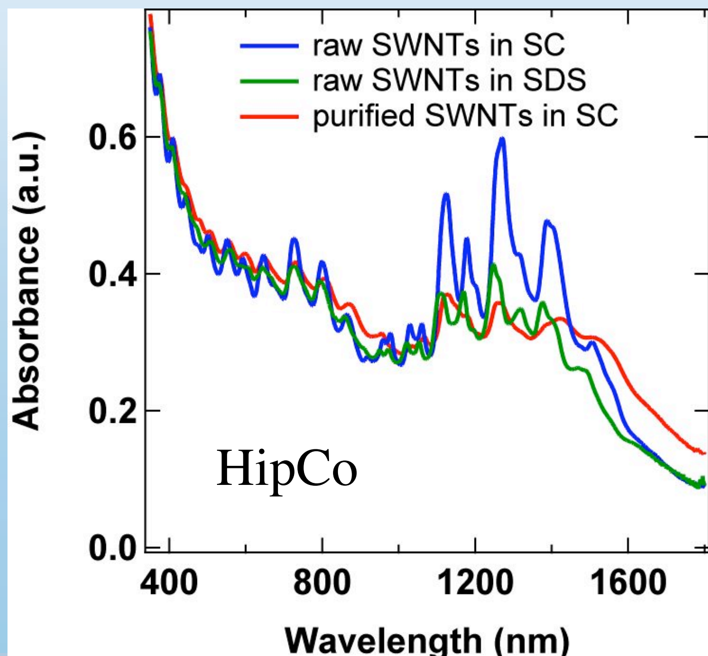

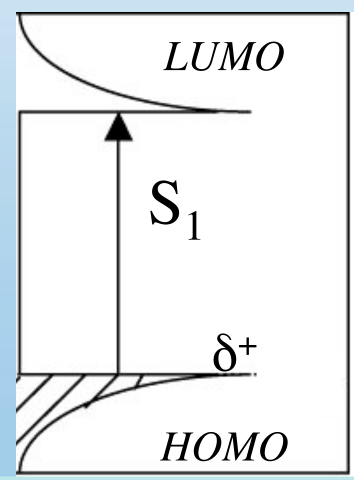

Enhanced Auger recombination with acid doping? [1]

[1] Dukovic et al., JACS 2004

Changes in the Branching Ratio for E_{2-1}

Purified HipCo Deprotonated with H_2O_2

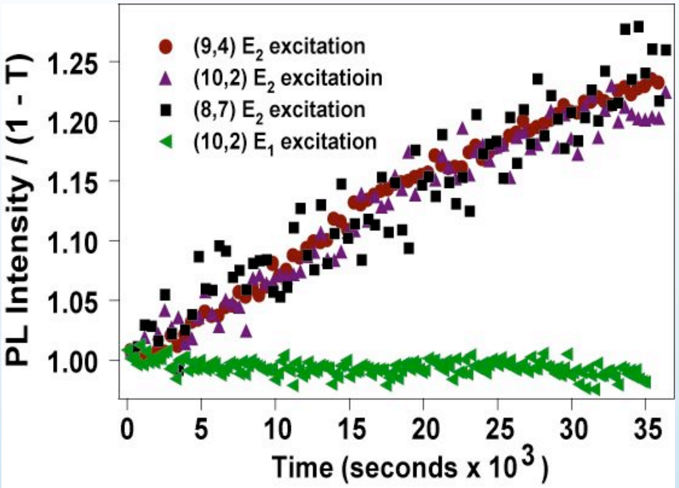

PL Excited at E_1

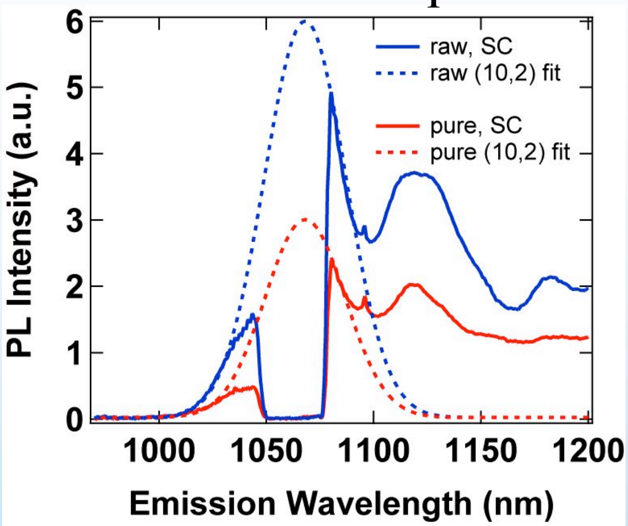

Ma et al, *J. Phys. Chem. B* **2005**, *109*, 15671.

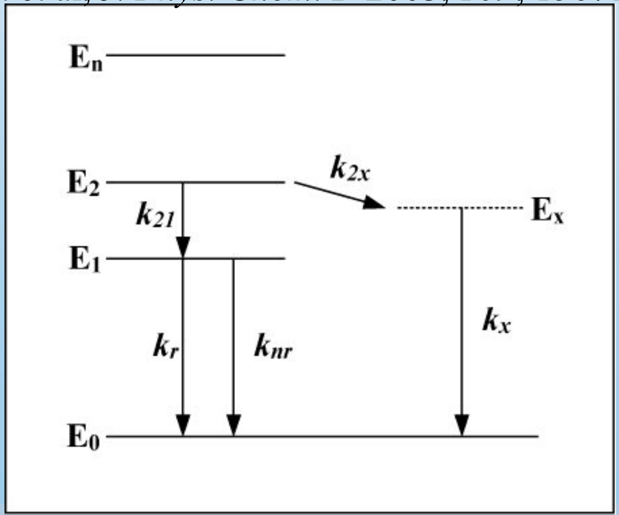

Photoluminescence Quantum Yield

$$\phi_{PL} = \frac{k_r}{\sum_{i=0}^{j} k_i} = \frac{k_r}{k_r + k_{nr}}$$

Branching Ratio for E_{21} Relaxation

$$\phi_{21} = \frac{k_{21}}{\sum_{i=0}^{j} k_i} = \frac{k_{21}}{k_{21} + k_{2x}}$$

(2) Where do the Orbitals Sit versus Vacuum?

Do tube Fermi levels move substantially with diameter?

Okazaki et al., PRB 68, 035434 (2003)

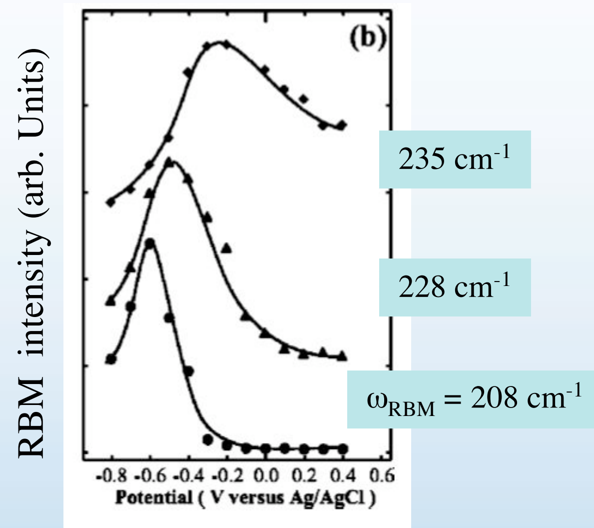

- Raman study of SDS-dispersed SWNTs on potential-controlled electrode in aqeous solution.
- RBM intensity variation measured as function of voltage determines position of vH singularities and E_f *vs* reference electrode.
- Measurements indicate E_f is a function of E_{ii}:
  - E_f / E_{ii} ~ 1.96 for semiconductors
  - Steeper dependence for metals

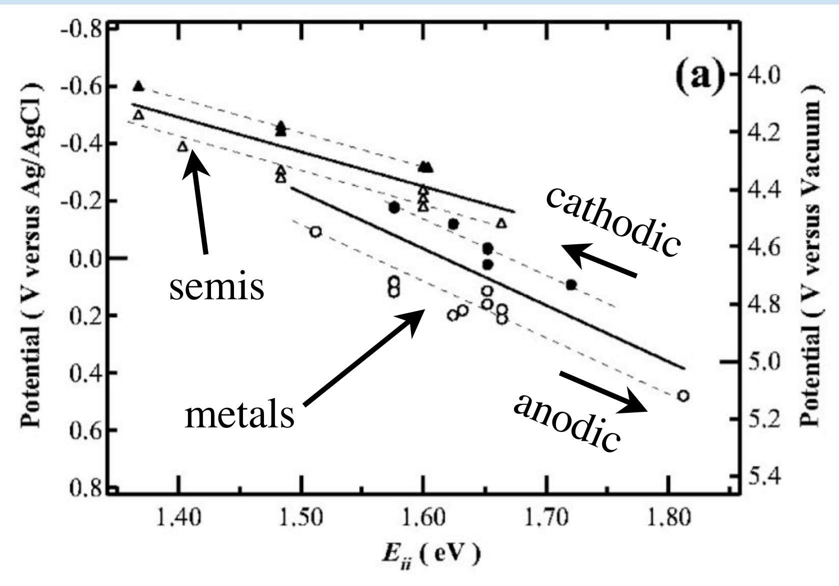

Chirality Dependent Charge Transfer Bleaching of PL[1]

Redox titration of DNA-wrapped tubes with K_2IrCl_6 permits absolute referencing of the HOMO of (6,5) tube,[2] and plotting of the energy levels of a wide range of tubes.[1]

Φ_{HOPG} ~ 4.6 eV

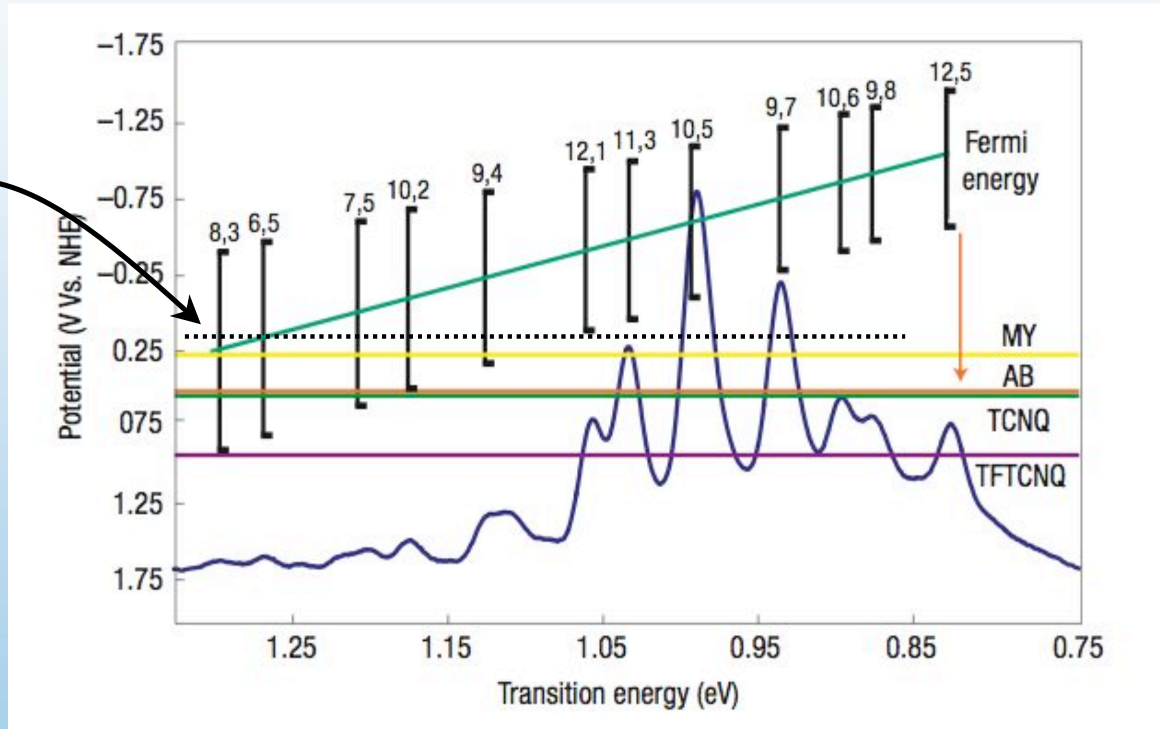

[1] O'Connell et al., *Nat. Mat.* **4** 412 (2005)

[2] Zeng and Diner, *JACS* **126** 15490 (2004)

E_f Expected to be ~Constant with Tube Diameter

- Zeng and Diner estimated a variation of ~50 meV in the v1 position for E_G range of 0.98 to 1.25 eV.
- DFT calculations for smaller tubes[1] and our own DFT calculations for these HiPCO tubes agree.

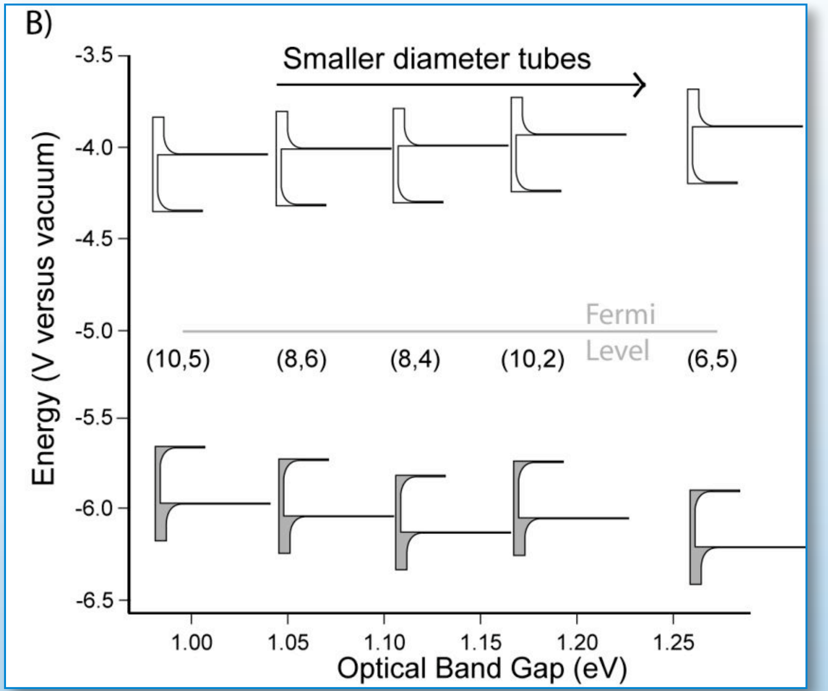

[1]Shan & Cho, PRL **94** 236602 (2005).

Two Very Different Pictures

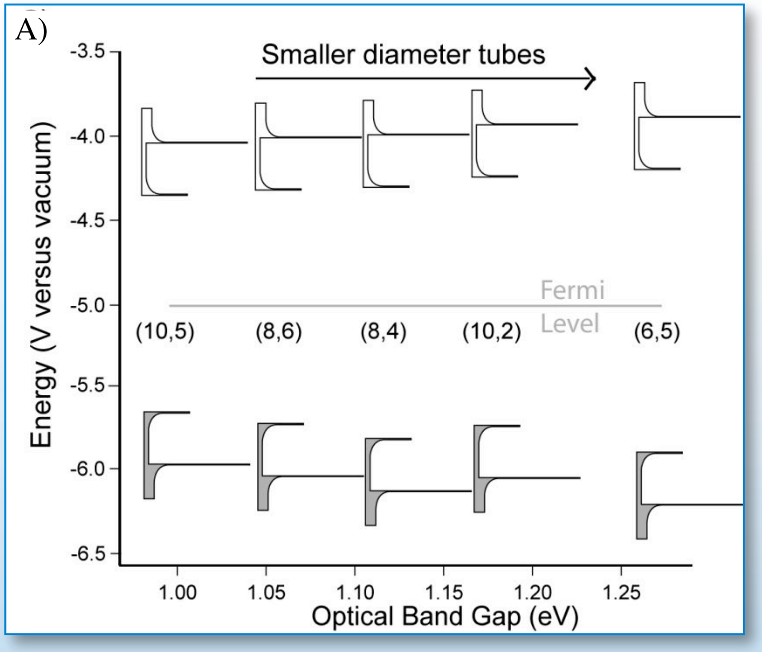

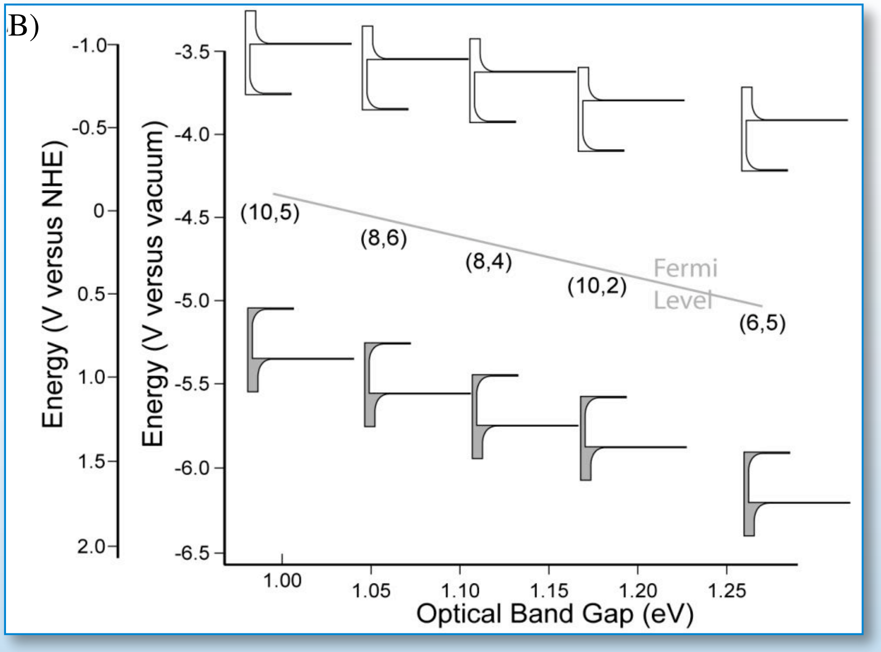

A. Experiments[1] with strongly bound DNA and theory[2] show that the NT Fermi level varies little as a function of bandgap.

B. Experimental studies with surfactants conclude that NT Fermi level is a strong, linear function of bandgap.[3,4]

1. B. Shan, K. Cho, *Physical Review Letters* **94**, 236602 (2005).
2. M. Zheng and B.A. Diner, *JACS* 126, 15490, 2004
3. K. Okazaki, Y. Nakato, and K. Murakoshi, *Physical Review B* **68** (3) (2003).
4. M. J. O'Connell, E. E. Eibergen, and S. K. Doorn, *Nature Materials* **4** (5), 412 (2005).

Surfactant “Binding Energies” Vary with Tube Diameter

McDonald, et al. *JPCB* **2006**, ***110***, 25339.

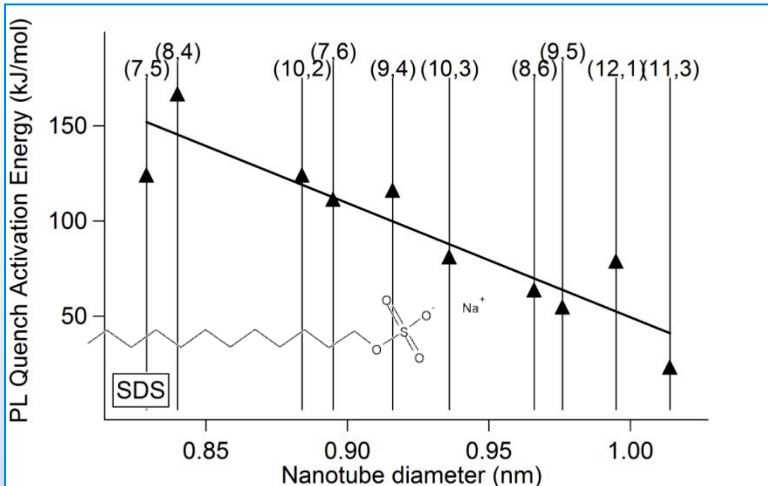

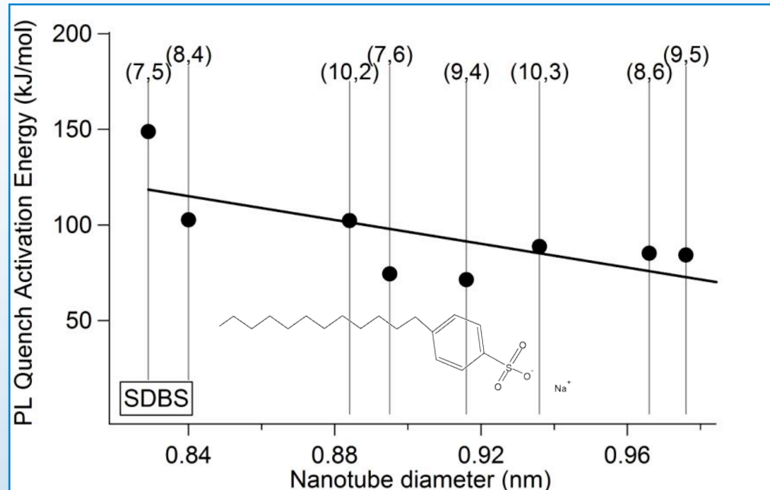

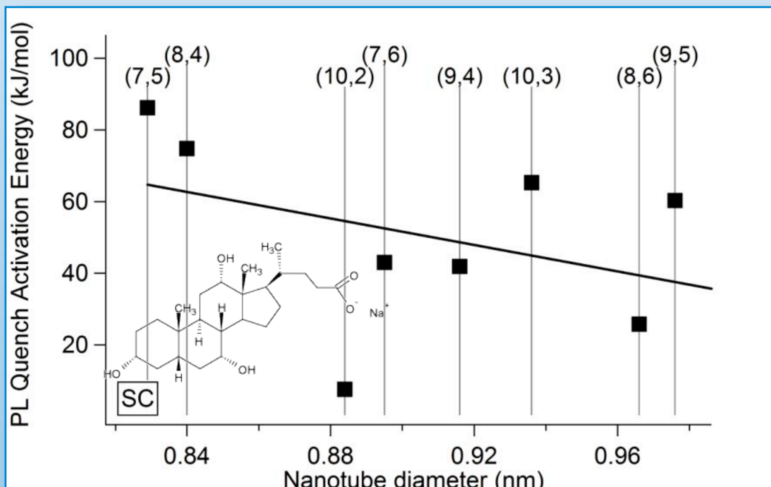

Any relation to dependence reported by Okazaki et al. and O’Connell et al?

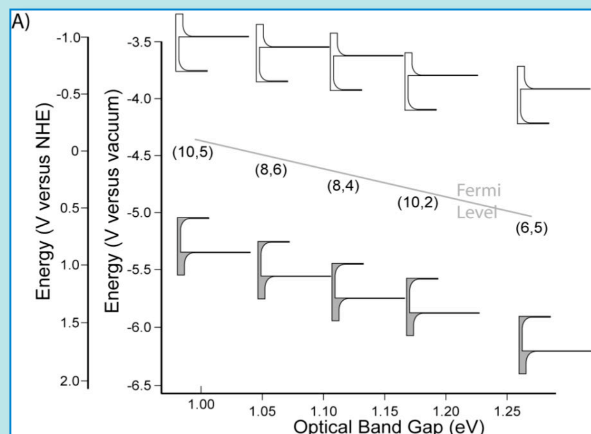

Surfactant Dynamics in Suspensions

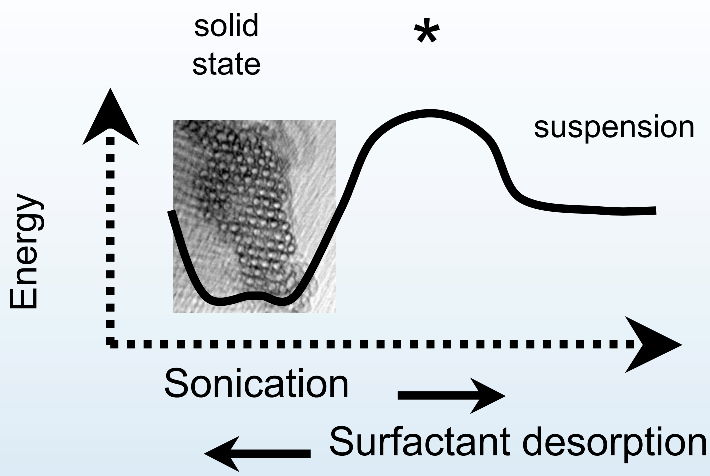

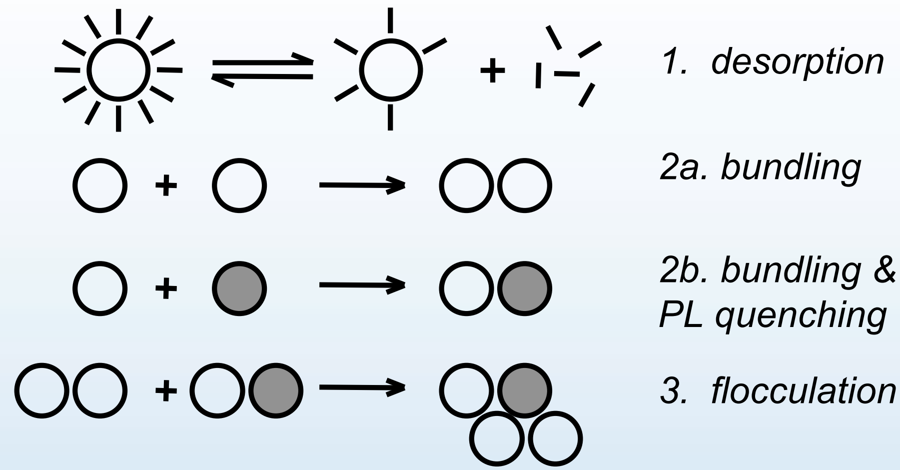

McDonald, et al. *JPCB* **2006**, ***110***, 25339.

[SDBS] diluted from 5 cmc to 1/3 cmc

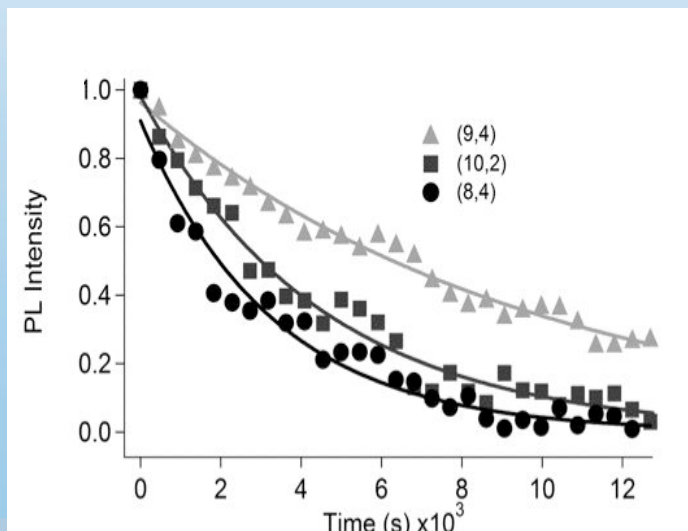

As f(T) with SDS dilution

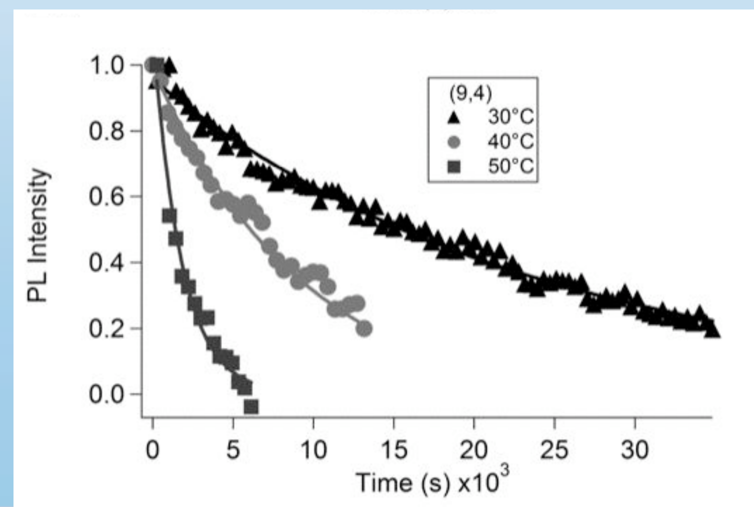

Origin of Similarity in Data Sets

1. Smaller D, large E_G tubes bind surfactant more strongly

2. Small D tubes more completely sheathed
   - surface is less accessible to, e.g., redox species

3. Diameter dependent kinetics of PL quenching can be ascribed to different available effective surfaces areas.
   - $A_{eff,\ small\ D} < A_{eff,\ large\ D}$

Bottom line for this view:

Large D: Good kinetics (controlled by energetics)

Small D: Poor kinetics (controlled by mass transport)

Surface-bound Redox Link to SWNT with Hydrogenase

- Complexes comprised of the [FeFe] hydrogenase I from the anaerobic bacterium *Clostridium acetobutylicum* and SWNTs form spontanetously in cholate solutions.
- When assembled under reducing and proper conditions, the SWNTs become sensitive to the hyrogen half reaction: $2H^+ + 2e^- \leftrightarrows H_2$

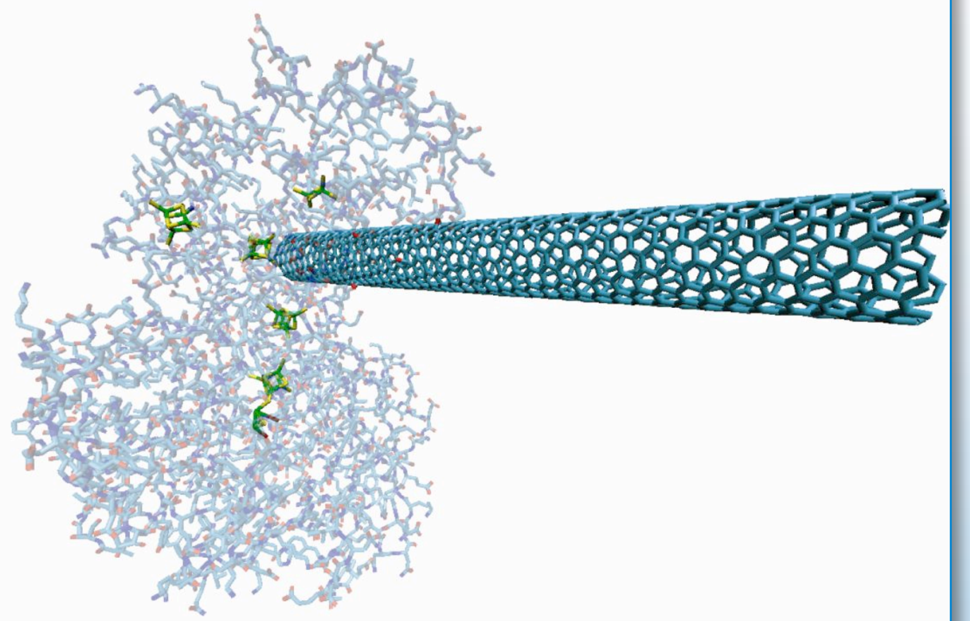

http://bioinfo3d.cs.tau.ac.il/PatchDock/patchdock

- Enzymes comprised of polypeptide chains and first-row transition metals
- The biological activation of H_2 is accomplished through these metalloenzymes that catalyze the reaction: $2H^+ + 2e^- \leftrightarrows H_2$
- Challenge for “wiring-up” the enzyme is to establish electrical connection

McDonald et al., *Nano Lett.*, **2007**, *7* (11), pp 3528–3534

PL is Quenched as Hyd-NT Complexes Form

PL from (7,6) nanotube

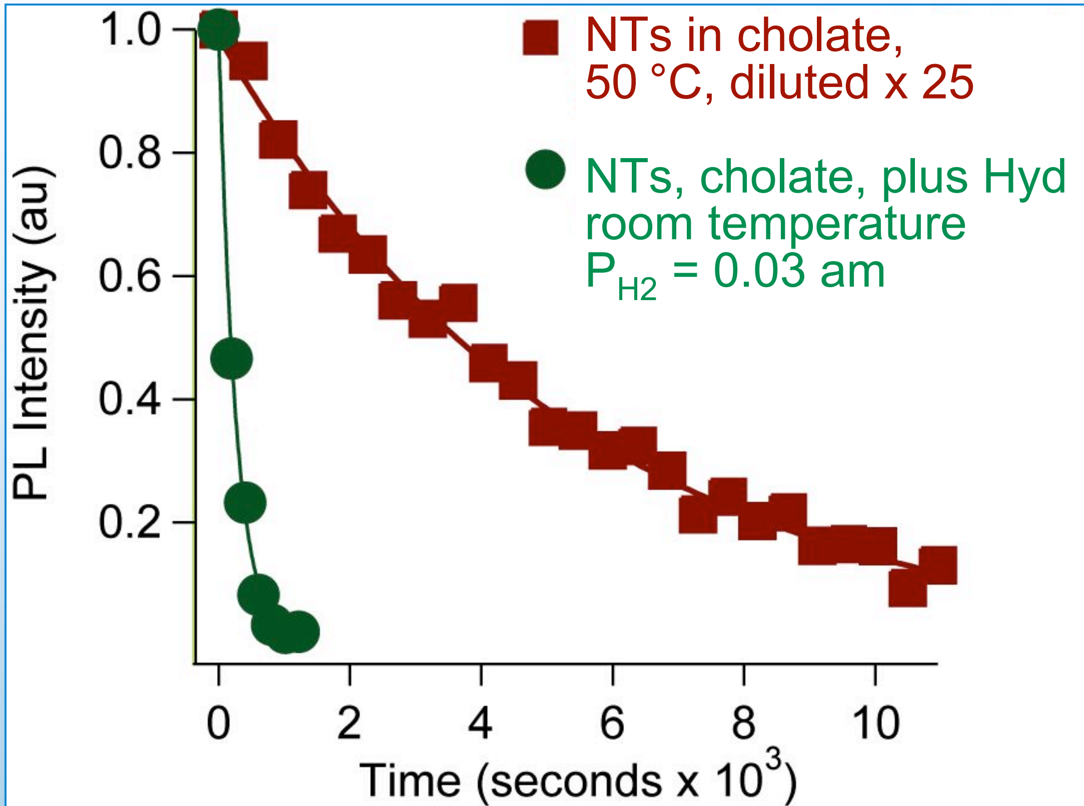

- Hyd adsorbs more strongly and displaces NaCholate
- Effect not seen if anaerobic (reducing) conditions are not maintained

McDonald et al., Nano Lett., 2007, 7 (11), pp 3528-3534

Absorption Spectra Before and After Hyd Addition

- Reduction of E_1 oscillator strength suggestive of electron transfer to SWNTs
- Higher lying transitions not significantly affected.
  - no gross structural changes

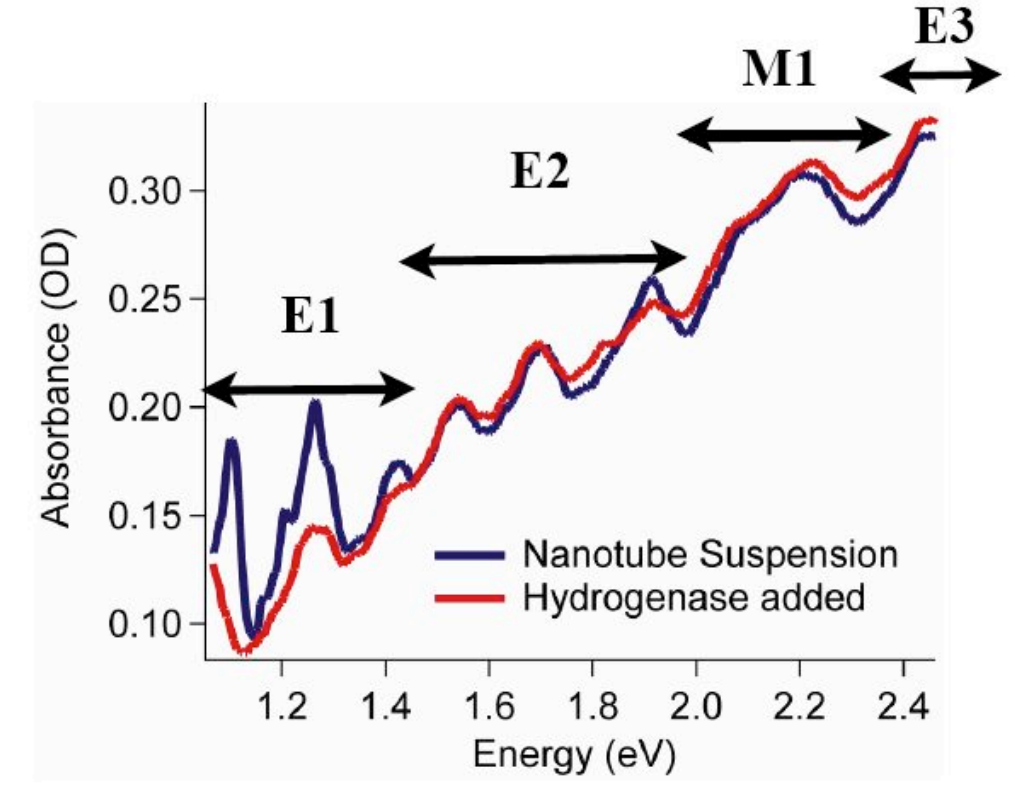

McDonald et al., Nano Lett., 2007, 7 (11), pp 3528-3534

PL Maps Become Sensitive to PH_2

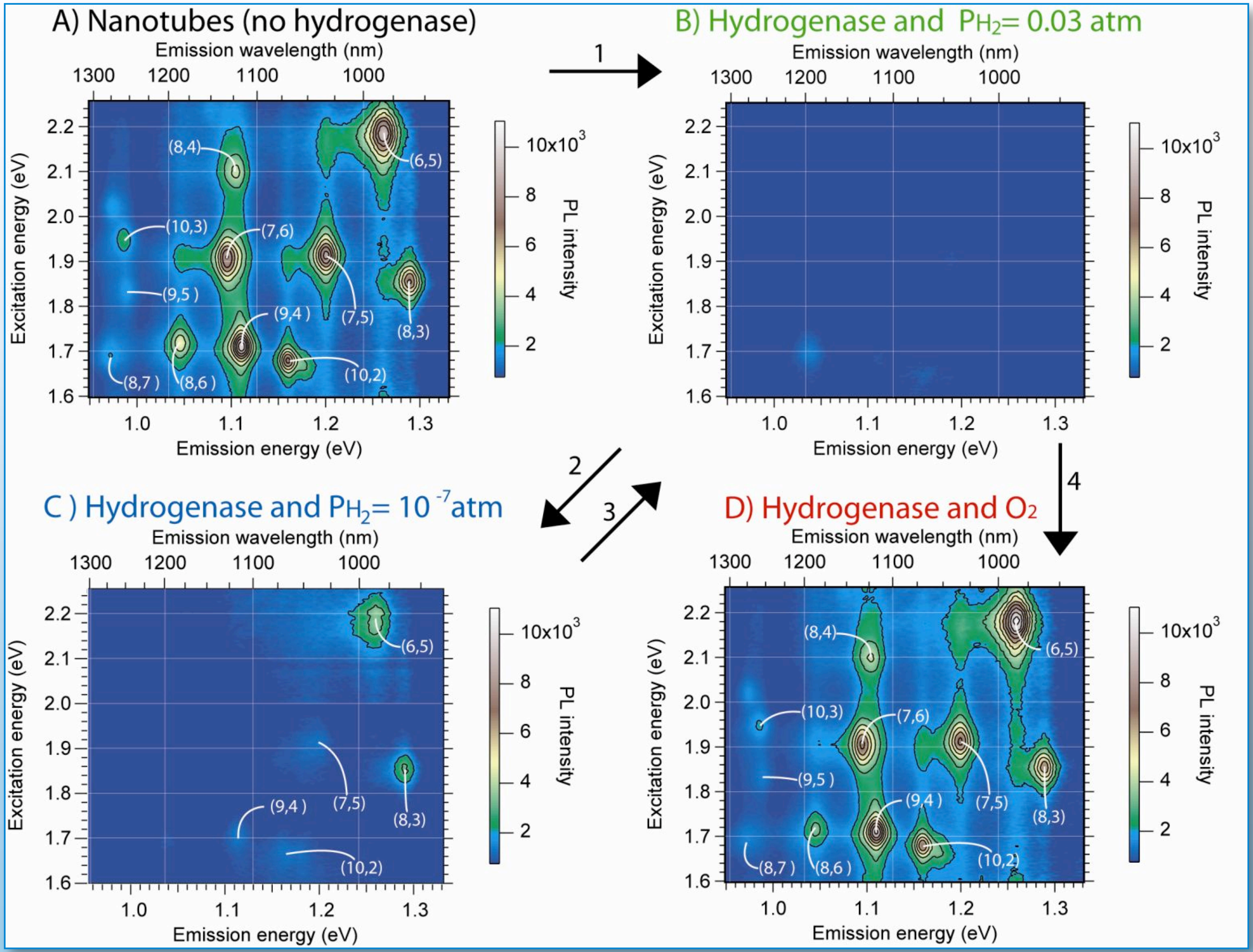

McDonald et al., Nano Lett., 2007, 7 (11), pp 3528-3534

Energy Level Titration

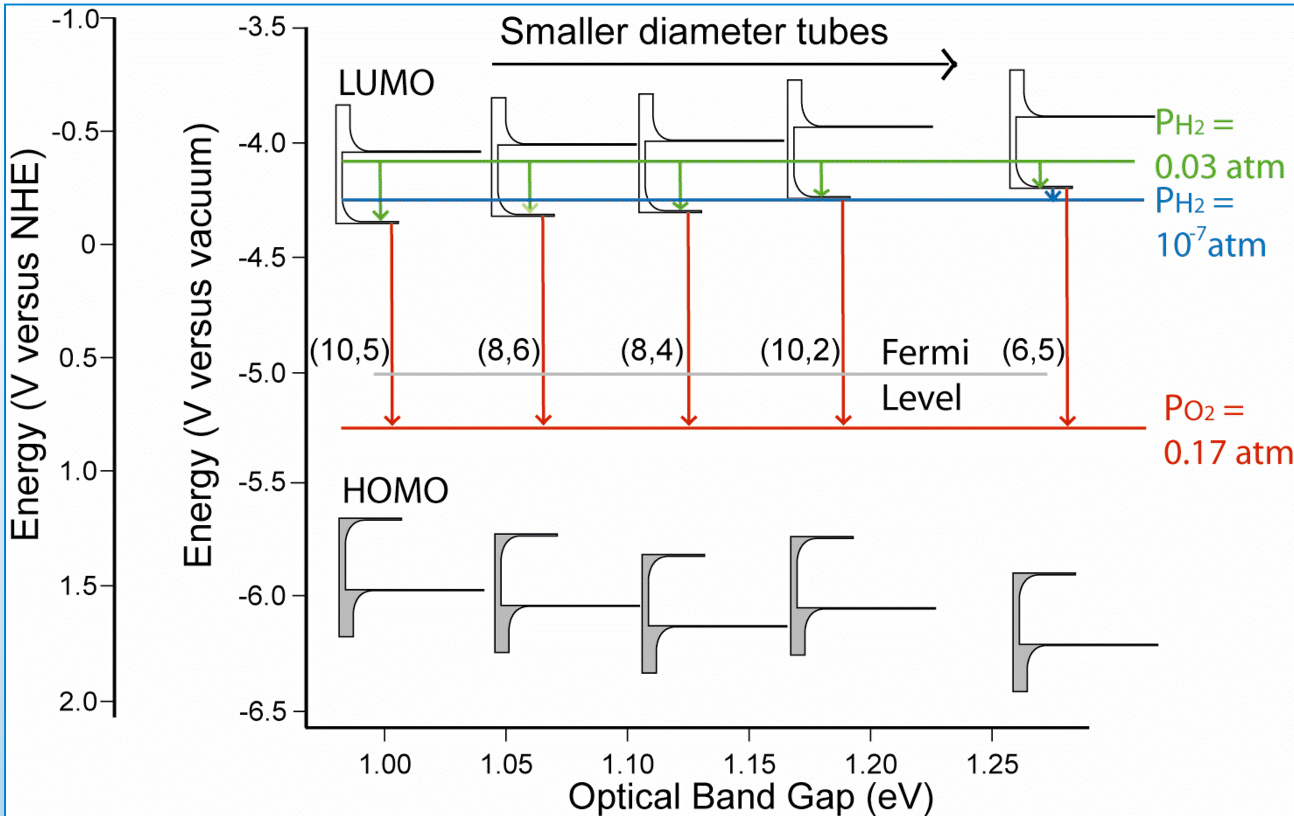

- Energy level locations probed with $2H^+ + 2e^- \leftrightarrows H_2$ redox couple
- Locations as expected from DFT-LDA
- Consistent with Zheng & Diner and Shan & Cho

McDonald et al., Nano Lett., 2007, 7 (11), pp 3528-3534

(3) Separating Metallic and Semiconducting SWNTs by Density Gradient Centrifugation

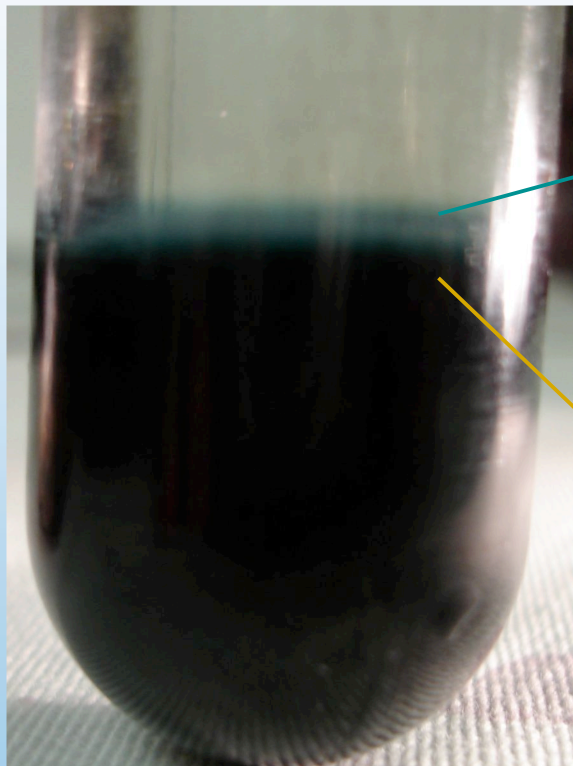

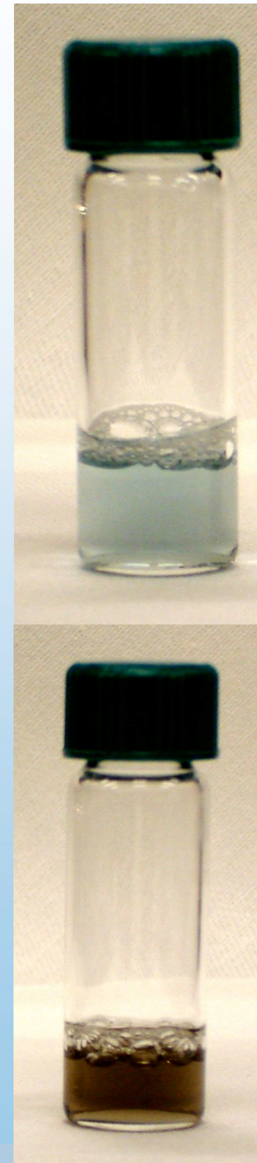

m-SWNTs

s-SWNTs

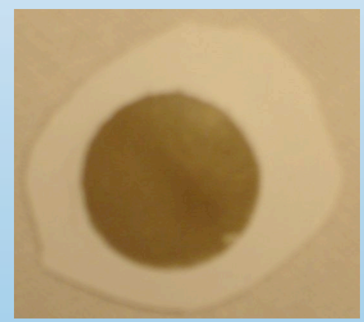

Arnold, *Nature Nanotech*. **1**, 60 (2006)

Absorbance Spectra of Separated Films

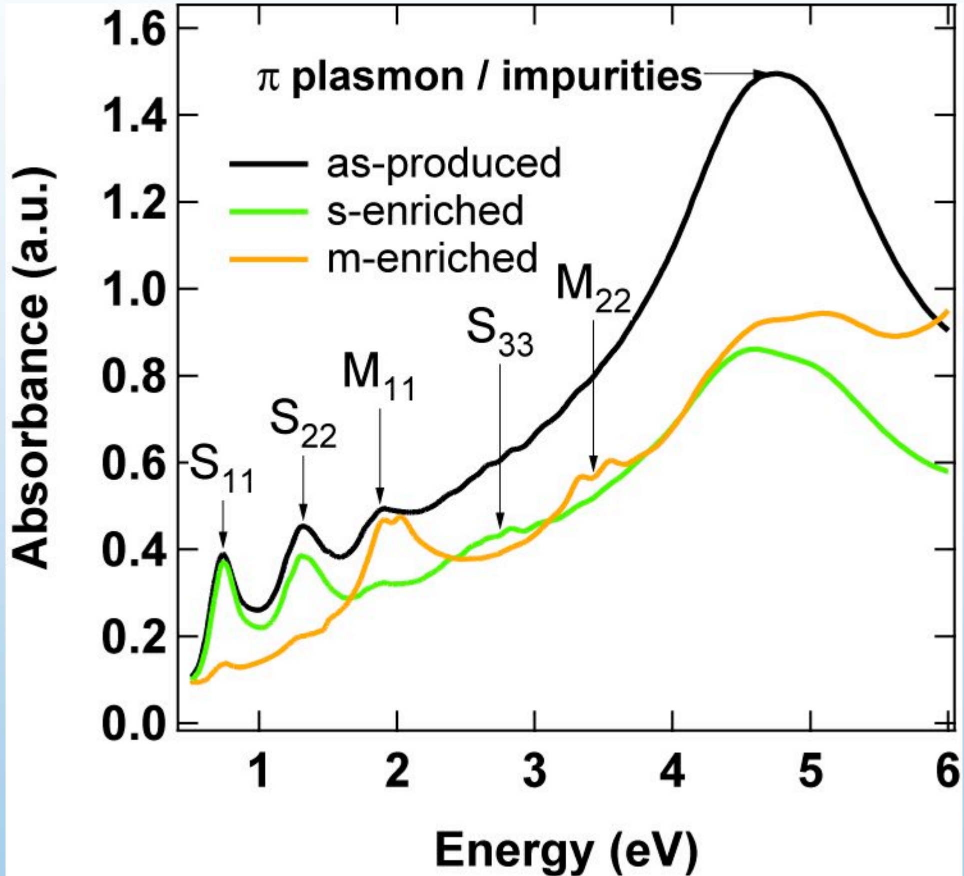

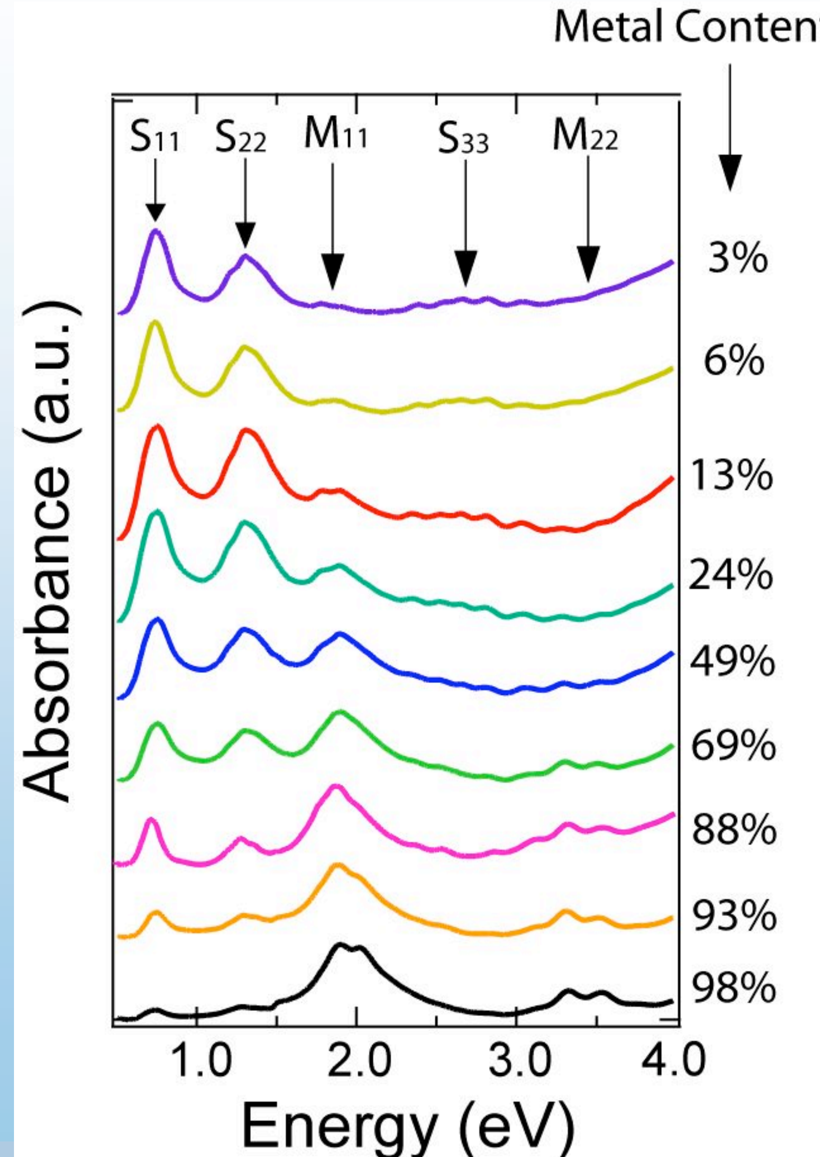

Blackburn, et al., *ACS Nano*, **2008**, 2 (6), pp 1266–1274